# Review: Recent advances of one-dimensional coordination polymers as catalysts

Article (Accepted Version)

# Recent advances of one-dimensional coordination polymers as catalysts

Edward Loukopoulos[a] and George E. Kostakis [a]*

[a]Department of Chemistry, School of Life Sciences, University of Sussex, Brighton BN1 9QJ, UK.

e-mail: G.Kostakis@sussex.ac.uk

## 0. LIST OF ABBREVIATIONS

0D = zero-dimensional
1,4-DHPs = 1,4-dihydropyridine
1D = one-dimensional
2,4-DNP = 2,4-nitrophenol
2D = two-dimensional
2L-$H_2$asp = N-(2-pyridylmethyl)-L-aspartic acid
3D = three-dimensional
3L-val = N-(3-pyridylmethyl)-L-valine
aq. = aqueous
bbbi = 1,1'-(1,4-butanediyl)bis-1H-benzimidazole)
bbmb = 1,2-bis((1H-benzo[d][1,2,3]triazol-1-yl)methyl)benzene
bdob = 1,4-bis(4,5-dihydro-2-oxazolyl)benzene
bipy = 4,4'-bipyridine
bm = benzimidazole
[(bmim)($BF_4$)] = 1-butyl-3-methylimidazolium tetrafluoroborate
BMPyr = 1-butyl-1-methylpyrrolidinium
btSe = benzene-1,2,4,5-tetraselenolate
btt = benzene-1,2,4,5-tetrathiol
CP = coordination polymer
CR = Congo Red
Cy = cyclohexane
dfbi = 1,1'-(9,9-dimethyl-9H-fluorene-2,7-diyl)bis(1H-imidazole)
D-$H_2$pen = D-penicillamine
DMF = N,N-dimethylformamide
DMSO = Dimethylsulfoxide
dped = 1,2-bis(diphenylphosphino)ethane dioxide
dpppda = 1,4-N,N,N′,N′-tetra(diphenylphosphanylmethyl) benzene diamine
ee = enantiomeric excess
ESI-MS = electrospray ionization mass spectrometry
EtOH = ethanol
FTIR = Fourier-transform infrared spectroscopy
Hbmmp = 4-ethyl-2,6-bis((E)-((3-morpholinopropyl)imino)methyl)phenol
HPNP = 2-hydroxypropyl-*p*-nitrophenylphosphate
Htbba = 4-((4-([2,2':6',2"-terpyridin]-4'-yl)benzyl)oxy)benzoic acid
$H_2$aipa = 5-acetamidoisophthalic acid
$H_2$bipa = 5-benzamidoisophthalic acid

$H_2$bpdc = 4,4’-biphenyldicarboxylic acid
$H_2$cybps = 1,2-cyclohexanediamino-N,N’-bis(3-tert-butyl-5-(4-pyridyl)salicylidene
$H_2$dtda = 3,3″-dipropoxy-[1,1′:4′,1″-terphenyl]-4,4″-dicarboxylic acid
$H_2$hmb = 2-[(2-hydroxy-3-methoxyphenyl)methylideneamino]benzenesulfonic acid
$H_2$icyd = N,N’-bis-[(imidazol-4-yl)methylene]cyclohexane-1,2- diamine
$H_2$ntp = 2-nitroterephthalic acid
$H_2$phba = 4-hydroxybenzoic acid
$H_2$ppd = bis(pyridin-2-ylmethylene)pyridine-2,6-dicarbohydrazide
$H_2$pydca = pyridine-2,6-dicarboxylate
$H_2$tae = 1,1,2,2-tetraacetylethane
$H_3$bes = N,N-bis(2-hydroxyethyl)-2-aminoethanesulfonic acid
$H_3$btc = 1,2,4-trimellitic acid
$H_3$ccb = 3-(carboxymethyl-amino)-4-chlorobenzoic acid
$H_3$cia = N-(4-carboxybenzyl) iminodiacetic acid
$H_3$dhia = 5-(2-(4,4-dimethyl-2,6-dioxocyclohexylidene)hydrazinyl)isophthalic acid
$H_3$dht = 2-(2-(4,4-dimethyl-2,6-dioxocyclo-hexylidene)hydrazinyl)terephthalic acid
$H_3$dmb = 2-[(2,3-dihydroxyphenyl)methylideneamino]benzenesulfonic acid
$H_3$tea = triethanolamine
$H_4$bccy = N,N′-bis(4-carboxysalicylidene)cyclohexanediamine
$H_4$bced = N,N’-bis(4-carboxysalicylidene)ethylenediamine
$H_4$hpd = bis(2-hydroxybenzylidene)pyridine-2,6-dicarbohydrazide
$H_4$pdada = 4,4'-((pyridine-2,6-dicarbonyl)bis(azanediyl))dibenzoic acid
$H_4$pma = pyromellitic acid
$H_6$bmt = (benzene-1,3,5-triyltris(methylene))triphosphonic acid
$H_6$nmp = nitrilotris(methylenephosphonic acid)
IL = ionic liquid
iPrOH = 2-propanol
MB = methylene blue
MeCN = acetonitrile
MeOH = methanol
MO = Methyl Orange
MOF = metal–organic framework
MW = microwave
NB = nitrobenzene
NMF = N-Methylformamide
$NTf_2$ = bis(trifluoromethanesulfonyl)imide
PhIO = iodosobenzene
pmba = 2-(2-pyridylmethyleneamino)benzenesulfonic acid
PNP = paranitrophenol
RhB = Rhodamine B
TBHP = *tert*-Butyl hydroperoxide
THF = Tetrahydrofuran
TFA = Trifluoromethanesulfonic acid
TMSCN = Trimethylsilyl cyanide
tpb = N,N,N-tris(3-pyridinyl)-1,3,5-benzenetricarboxamide
tppz = 2,3,5,6-tetrakis(2-pyridyl)pyrazine

UV-Vis = ultraviolet–visible spectroscopy
XPS = X-ray photoelectron spectroscopy

## 1. INTRODUCTION

Throughout the numerous amount of studies performed in the fields of Inorganic and Coordination Chemistry during the last 50 years, research on infinite, hybrid organic-inorganic compounds, Coordination Polymers (CPs) holds a leading position. CPs are constructed from metal centers linked to each other via organic ligands (linkers) through coordination bonds, thus forming structures that extend into one, two or three dimensions[1,2].

While the term of "coordination polymer" has been regularly used in scientific reports since the 1950s[3], interest in this field exploded rapidly in the early 1990s (Scheme 1) when Hoskins, Robson and others published a series of papers[4–9] proposing a design approach towards CPs with targeted structures. The development of this concept was further aided by the rising growth of crystal engineering, which concerns the study and understanding of intermolecular interactions (eg. hydrogen bonds, halogen bonds, $\pi\cdot\cdot\pi$ interactions etc.) in a crystal structure, towards the design of new molecules with desired applications[10–12]. These concepts have been widely used for the production of CPs ever since[13]: synthetic variables such as metal salt[14,15] and ligand selection[16–18], or solvent[19–22] and temperature[23–25] conditions may be controlled and manipulated to afford polymeric compounds with the desired shape and dimensionality, and most importantly the desired applications. As a result, a large number of CPs has been reported with potential properties in anion exchange[26,27], crystal-to-crystal transformation[28–31], gas sorption[32,33], drug delivery[34,35], luminescence[36,37], magnetism[38], sensing[39,40] and catalysis[41].

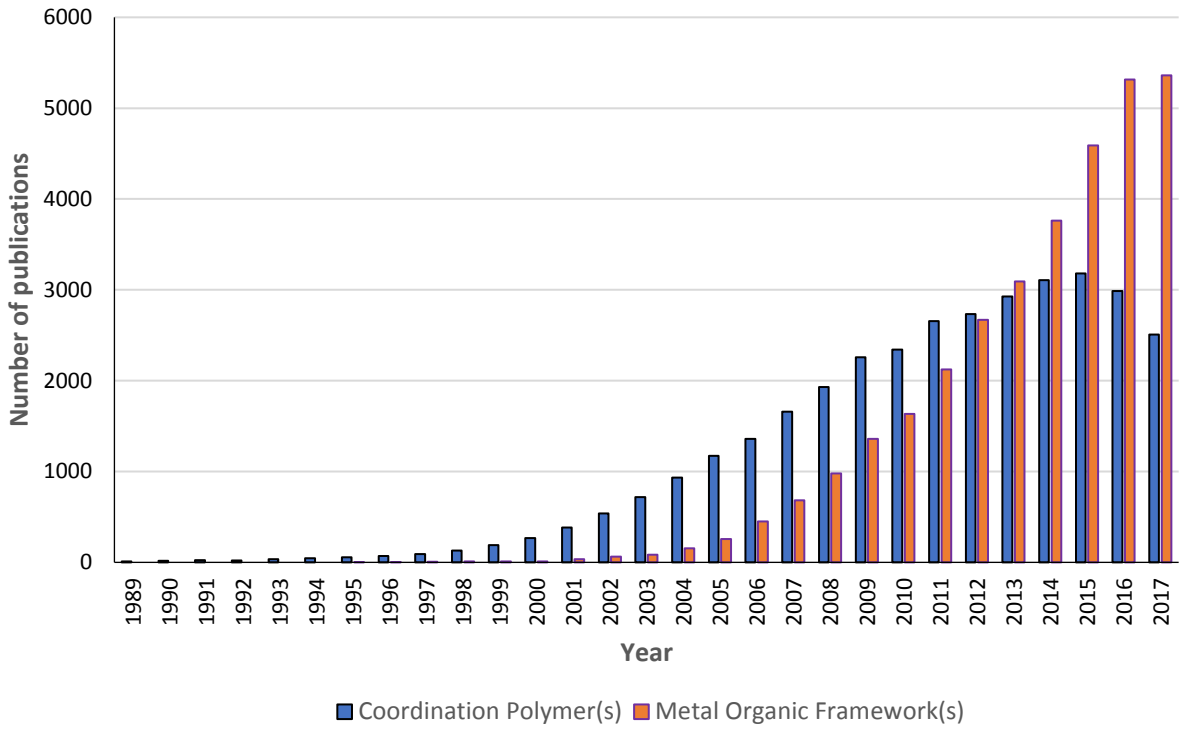


**Scheme 1.** Number of publications per year on the topics of "coordination polymer(s)" or "metal organic framework(s)". Based on a Web of Science search (November 2017).

A large majority of these studies refer to porous three-dimensional (3D) CPs, which are also known as metal–organic frameworks (MOFs), a term popularized by Yaghi et al. in 1995[42,43]. However, more efforts to systematically study the potential properties of lesser-dimensional CPs have been made recently[44–50]. Despite their structural simplicity compared to MOFs, one dimensional (1D) CPs in particular are generally easier to synthesize and the resulting framework can be tuned more effectively in order to generate structures with maximized application potential[51,52]. A number of detailed reviews regarding the potential of 1D CPs have been published. In 1993 Chen and Suslick[53] reported the uses of 1D CPs in various topics of materials science. In 2011, a comprehensive review by Leong and Vittal[54] covered the literature on 1D CPs from 1993 up to the end of the previous decade, focusing on structural motifs and supramolecular architecture issues as well as their applications. More recently, a study by Slabbert and Rademeyer[55] published in 2015 focused on the structural trends of 1D halide-bridged CPs. In all cases, the catalytic properties of 1D CPs received lesser focus; however, efforts towards more systematic studies in this field have been made recently. 1D CPs can catalyze an organic transformation via homo- or

heterogeneous pathways depending on their solubility; this can introduce ambiguity when determining the active catalytic species and is therefore considered as a disadvantage when compared to the capabilities of 3D porous MOFs. On the other hand, their easy synthesis and tuning offers greater potential and unrivaled variability for mechanism unraveling or catalyst development in an existing system. Therefore, 1D CPs with catalytic activity present a unique opportunity to connect Inorganic and Organic Chemistry, providing invaluable information. This has led to an increased number of relevant reports in the literature.

This review aims to provide reports of 1D CPs that have been used as catalysts in various organic reactions in the last decade, covering the literature from 2007 and onwards. The CPs have been mainly categorized into homometallic and heterometallic compounds; additional parameters such as the metal and ligand selection for the CP are discussed, to provide a more detailed look into each system.

## 2. HOMOMETALLIC CPs

Several cases of 1D CPs with catalytic activity in oxidation reactions have been reported. Such reactions are a very useful tool for synthetic organic chemists, however due to the high activation energies involved they often require the use of a catalyst as well as harsh conditions. The first related compound was introduced in 2008 by Karabach and co-workers[56], synthesized through the self-assembly of Cu(II) nitrate, triethanolamine ($H_3$tea) and pyromellitic acid ($H_4$pma) in aqueous medium. The ligand selection was intended to promote the synthesis of CPs with a targeted Cu(II) coordination environment to mimic the respective environment in methane monooxygenase, a copper enzyme that can catalyze the oxidation of alkanes. Indeed, the resulting compound, $[Cu_2(tea)_2(pma)]$ (**1**), forms 1D ladder-like polymeric chains in which each Cu center possesses a $\{NO_5\}$ coordination environment (Figure 1). **1** was used as a catalyst precursor in the mild oxidation of cyclohexane (Scheme 1) at room temperature and in MeCN/$H_2O$, providing moderate conversion to cyclohexanol and cyclohexanone (29% overall yield based on cyclohexane); this result was comparable to other copper catalysts for this reaction. The catalyst was also found to largely retain its activity when reused in the reaction (26% overall yield after three recycles). Subsequently in 2014, Jlassi and others[57] introduced a series of Cu(II) compounds with catalytic activity in the same reaction. Among these compounds, a 1D zig-zag CP (Figure 2) formulated as $[Cu_2(H_2O)_2(H_2dht)(dht)]$ (**2**), where $H_3$dht = 2-(2-(4,4-dimethyl-2,6-dioxocyclo-

hexylidene)hydrazinyl)terephthalic acid, was also identified as a potential catalyst. A moderate yield of cyclohexanol and cyclohexanone was achieved (17% overall, based on cyclohexane) when **2** was used at a concentration of $3 \cdot 10^{-3}$ mol $L^{-1}$, under the presence of either MeCN or the ionic liquid 1-butyl-3-methylimidazolium tetrafluoroborate, [(bmim)($BF_4$)]. However, it should be noted that the finite complexes of the study exhibited higher catalytic performance in the reaction. The authors suggest that the varying coordination environment of copper in each compound could affect the ease of access to the active sites of the catalyst and thus the catalytic performance.

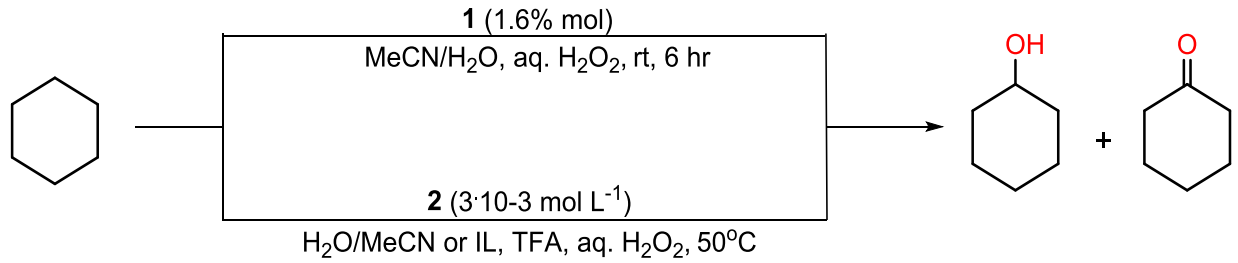


**Scheme 1.** Oxidation of cyclohexane catalyzed by **1** and **2**.

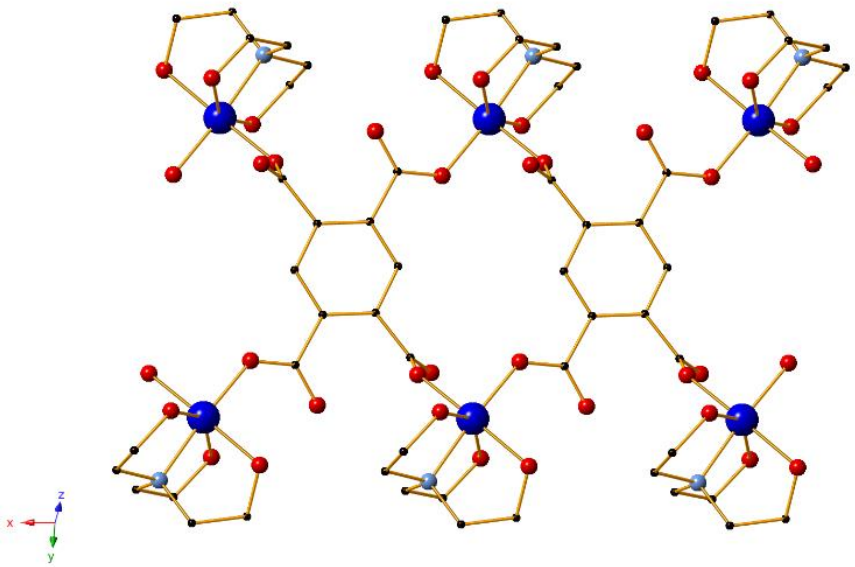

**Figure 1.** Part of the 1D architecture of **1**. H-atoms have been removed for clarity. Colour code Cu (blue), C (black), N (light blue), O (red).

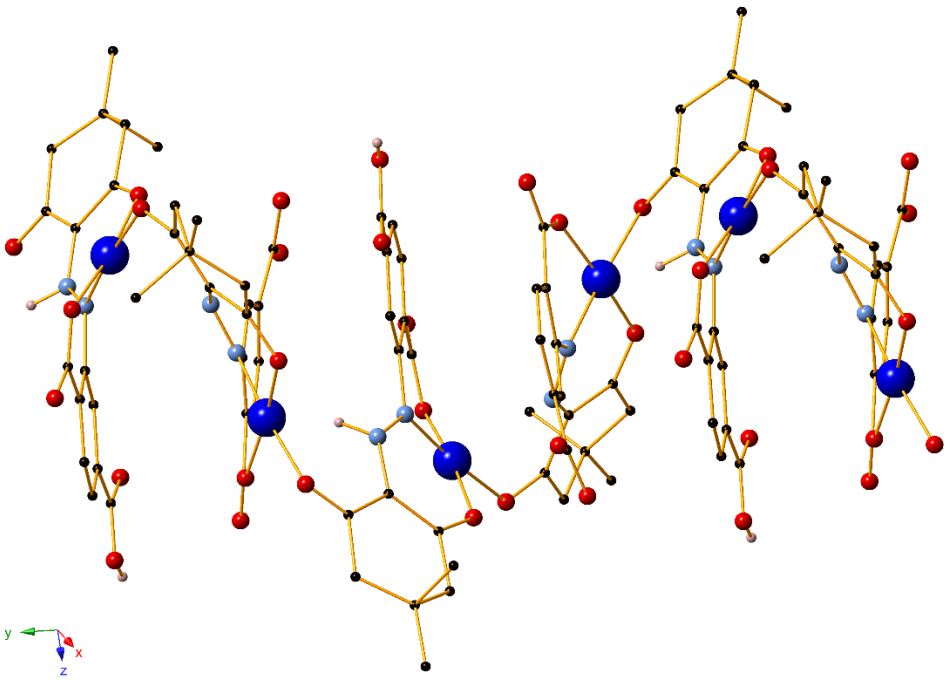

**Figure 2.** Part of the 1D architecture of **2**. Water molecules and certain H-atoms have been removed for clarity. Colour code Cu (blue), C (black), N (light blue), O (red), H (light pink).

In 2016, another Cu(II) 1D CP was reported by Paul and co-workers[58] towards oxidation of cyclohexane to the respective carboxylic acid. The authors employed a flexible terpyridine carboxylic acid derivative, 4-((4-([2,2':6',2"-terpyridin]-4'-yl)benzyl)oxy)benzoic acid (Htbba) to generate [Cu(tbba)($NO_3$)] (**3**), a 1D coordination polymeric chain with pentacoordinated Cu centers (Figure 3). Under the presence of the ionic liquid [BMPyr][$NTf_2$] (where [BMPyr = 1-butyl-1-methylpyrrolidinium, $NTf_2$ = bis(trifluoromethanesulfonyl)imide]) in aqueous medium, **3** can effectively catalyze the hydrocarboxylation of cyclohexane, producing the corresponding cyclohexanecarboxylic acid (Scheme 2) in 35.9% yield and in high selectivity. This one-pot conversion takes place under mild conditions and uses a low amount (0.8 mol%) of catalyst. Furthermore, the catalytic performance of **3** is maintained through four consecutive cycles after which a loss in the activity is observed.

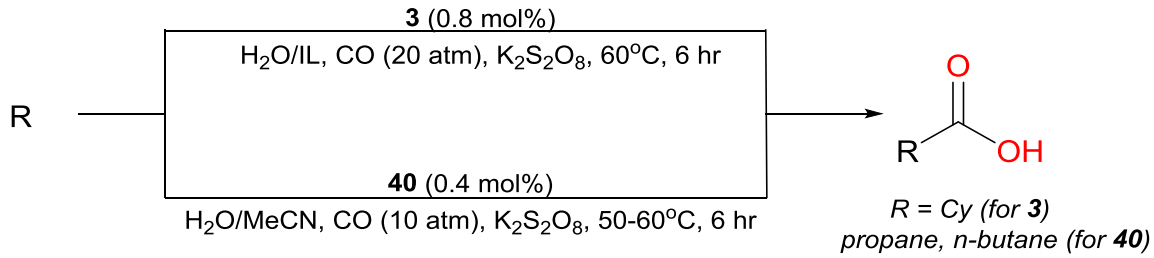


**Scheme 2.** Alkane oxidation to carboxylic acid catalyzed by **3** and **40**.

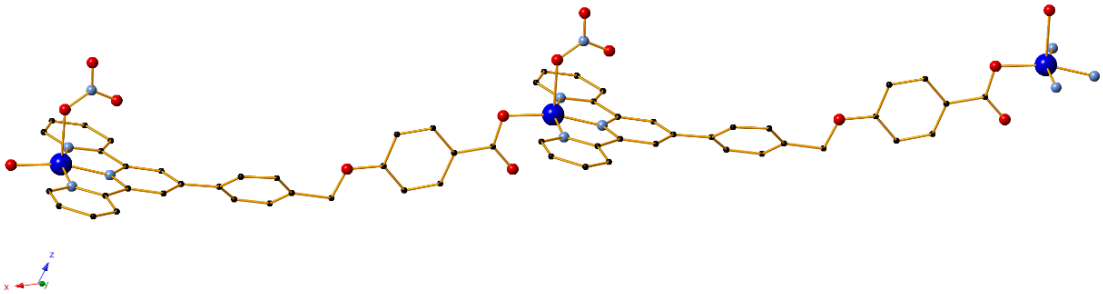

**Figure 3.** Part of the 1D polymeric chain in **3**. H-atoms have been removed for clarity. Colour code Cu (blue), C (black), N (light blue), O (red).

Very recently, Wang and co-workers[59] came up with a series of catalysts for the selective oxidation of arylalkanes to ketones. The synthetic procedure for the catalysts involves the use of various Cu(I) halogen sources and the tpb ligand (tpb = N,N,N-tris(3-pyridinyl)-1,3,5-benzenetricarboxamide). Out of the reported compounds, the iodine analogue formulated as [CuI(tpb)] (**4**) features a 1D framework along the *a* axis, which consists of a herringbone-like chain due to the conformation of the tpb molecules (Figure 4). Each Cu(I) center possesses a trigonal geometry and a $\{N_2I\}$ coordination environment. **4** acts as an excellent heterogeneous catalyst for the oxidation of a series of arylalkanes to the corresponding ketones (Scheme 3), providing the highest yields (72-99%) out of all the compared catalysts in the study. The ketones are afforded in very high selectivity and the reaction takes place under easy and eco-friendly conditions (air atmosphere, $H_2O$ as solvent, room temperature and only 4 hours stirring time). Additionally, only 5 mol% of the catalyst is employed, which can be then recovered and reused for at least six cycles with small losses in activity. Interestingly, the authors attribute the superiority of **4** to its coordination environment; it is proposed that the iodine anions enhance the activity of the metal centers and further facilitate the substrate binding.

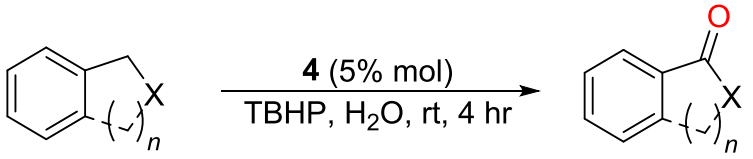


**Scheme 3.** Oxidation of arylalkanes to corresponding ketones as catalyzed by **4**.

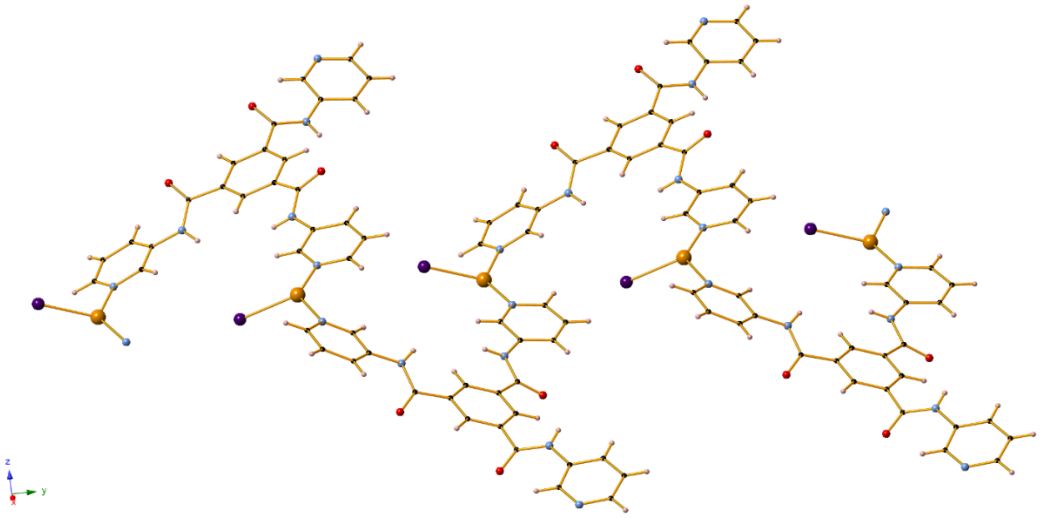

**Figure 4.** The 1D herringbone-like chain in **4**. Colour code Cu (light orange), C (black), N (light blue), O (red), I (purple), H (light pink).

Ever since the introduction of a Mn(II) salen-based coordination compound (also known as the Jacobsen catalyst[60,61]) with catalytic activity towards alkene epoxidation, more transition metal complexes have been explored to support this reaction[62–67]. In 2011, Huang and co-workers[68] incorporated 1D Ni(II) salen-based homochiral coordination polymers as self-supported heterogeneous catalysts in alkene epoxidation. These CPs were constructed in a two-step synthesis: First, the chirality of the compounds was functionalized through the use of salen-based R,R- or S,S-$H_2$cybps ($H_2$cybps = 1,2-cyclohexanediamino-N,N'-bis(3-tert-butyl-5-(4-pyridyl)salicylidene) as the main organic ligand. The resulting zero-dimensional Ni(cybps) coordination compounds were then used as nodes, as the use of 4,4'-biphenyldicarboxylic acid ($H_2$bpdc) as a secondary linker ensured the targeted synthesis of the 1D CPs [$Ni_3$(bpdc)(RR-cybps)$_2$]·DMF and [$Ni_3$(bpdc)(SS-cybps)$_2$]·DMF (**5** and **6** respectively). Both CPs are isostructural: Each chiral Ni(cybps) node coordinates to a terminal pyridyl group to form a helical chain which contains two Ni(cybps) units almost perpendicular to each other and a linking Ni-

bpdc component (Figure 5). The metal center of the Ni(cybps) units are unsaturated in both CPs and thus the compounds were identified as potential catalysts in alkene epoxidation. The reactions were carried out at room temperature under the non-coordinating solvent dichloromethane with 2 mol% of **5** or **6**. The catalytic activity of the compounds for styrene oxidation delivers moderate yields of the epoxide (21% for **5**, 19% for **6**), however the catalyst may be reused for at least two cycles before any loss in the activity is observed. For comparison, homogeneous counterparts were also synthesized, showing similar activity in the alkene epoxidation reaction.

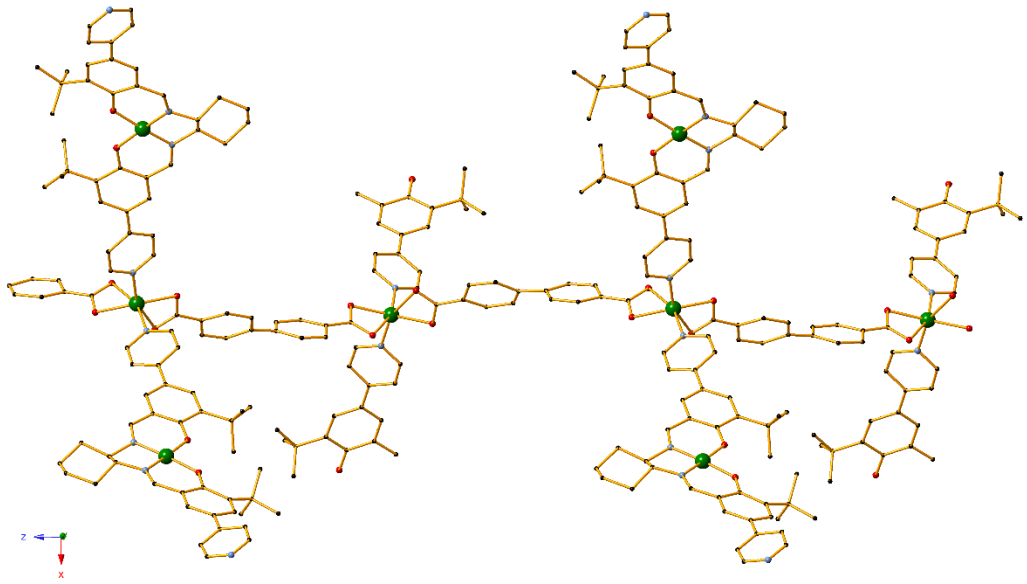

**Figure 5.** The 1D architecture in compound **5**. Lattice solvents and H-atoms have been removed for clarity. Colour code Ni (green), C (black), N (light blue), O (red).

Despite the success and popularity of Salen-based coordination compounds in this reaction, suitable compounds based on other ligands have also been proposed. A Mn(II) 1D CP with the ligand N-(4-carboxybenzyl) iminodiacetic acid ($H_3$cia) was reported in 2014 by Lymperopoulou[69] and co-workers, also showing catalytic activity in the epoxidation of alkenes. The compound, formulated as [Mn(Hcia)($H_2O$)] (**7**), forms 1D ladder-like chains with the ligand being only partially deprotonated (Figure 6), as the benzoic group remains intact and participates in H-bonding interactions. Catalysis-wise, **7** promotes the epoxidation of a large range of olefins when hydrogen peroxide and ammonium acetate were added respectively as oxidant and additive (Scheme 4). Typically the reactions proceeded under room temperature and were completed at 6

hours, providing epoxide products with moderate to high conversions (up to 81%) and excellent selectivities (up to 100%).

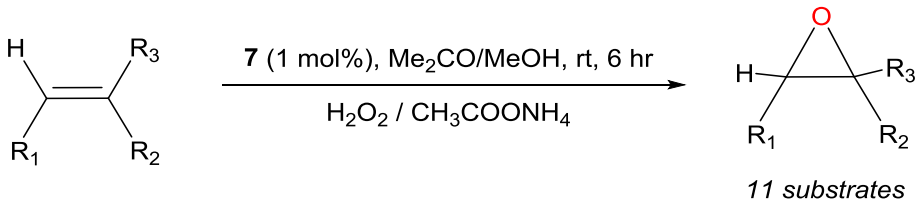


**Scheme 4.** Olefin epoxidation catalyzed by the 1D CP **7**.

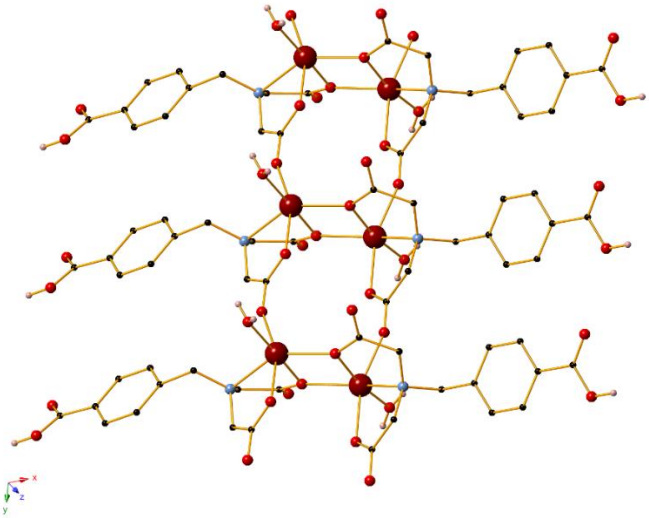

**Figure 6.** A view of the 1D ladder-like structure of **7**. Certain H-atoms have been removed for clarity. Colour code Mn (maroon), C (black), N (light blue), O (red), H (light pink)..

Other types of oxidation reactions have also been tested in order to untap the catalytic potential of 1D CPs. Recently, Martins and co-workers[70] introduced a new Sn(IV) coordination polymer which can act as a catalyst for the Baeyer–Villiger oxidation to convert linear and cyclic ketones to the respective ester and lactone products (Scheme 5). In this case, the catalyst design combines the coordination ability and potential catalytic activity of Sn(IV) centers with the versatility and easy synthesis of Schiff base ligands. For this reason, the compound is constructed using dimethyltin(IV) dichloride and the sulfonated Schiff base 2-[(2,3-dihydroxyphenyl)methylideneamino]benzenesulfonic acid ($H_3$dmb) as ligand. The resulting CP, formulated as [$SnMe_2$(Hdmb)(MeOH)]·0.5MeOH (**8**), extends to a zig-zag 1D framework through

bridging sulfonate groups (Figure 7). The ligand is only partially deprotonated, as the Sn(IV) center is not coordinated to the imine nitrogen atom of dmb. The heterogeneous catalytic behavior of **8** in the Baeyer–Villiger oxidation was then established for a variety of temperatures and procedures as simple stirring, microwave and ultrasound methods were tested under room temperature and 60°C for 1 hr. In all cases, hydrogen peroxide was used as the oxidant. The corresponding esters and lactones were afforded with good to excellent conversions up to 98%; the best results for most substrates were obtained under solvent-free ultrasound conditions and with only 0.1 mol% of **8**. Additionally, the reusability of the catalyst was verified for at least five cycles before any significant losses in conversion were observed.

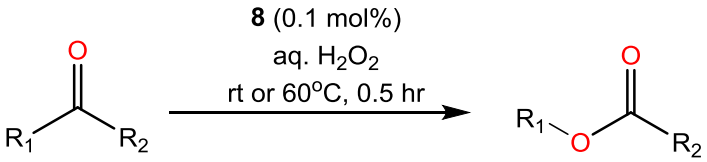


**Scheme 5.** Baeyer–Villiger oxidation as catalyzed by **8**.

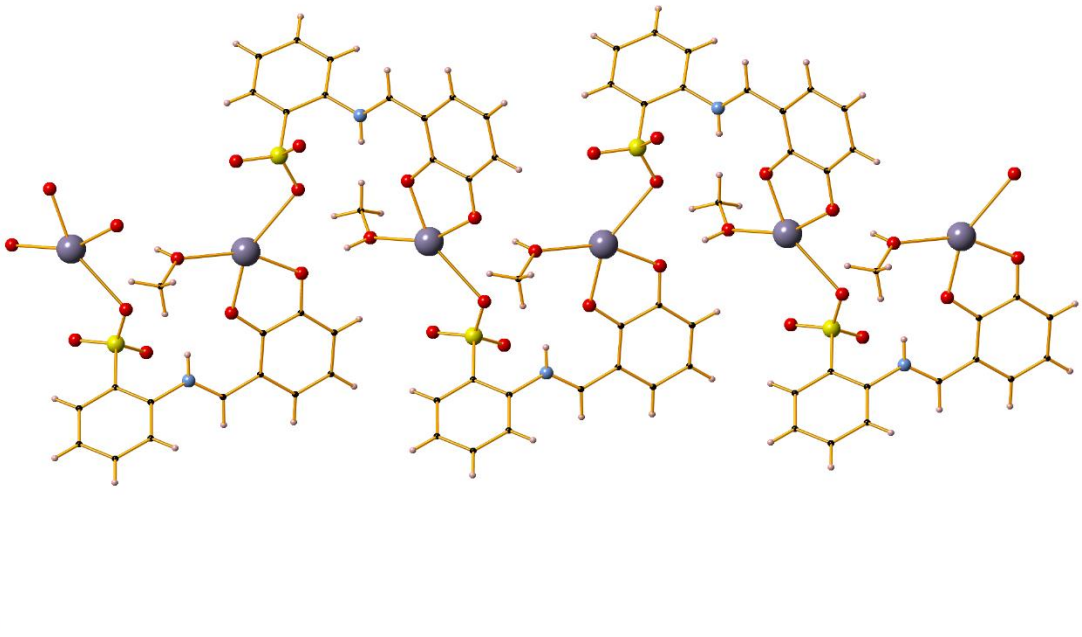

**Figure 7.** Part of the 1D zig-zag architecture of **8**. Solvent molecules have been removed for clarity. Colour code Sn (grey), C (black), N (light blue), O (red), S (yellow), H (light pink)..

Additional examples of catalysts based on Schiff base ligands have been reported. Very recently Hazra[71] and co-workers utilized 2-[(2-hydroxy-3-methoxyphenyl)methylideneamino]benzenesulfonic acid ($H_2$hmb), another sulfonated Schiff Base ligand in order to generate Cu(II) compounds. Compared to the previously mentioned $H_3$dmb which derived from 2,3-dihydroxybenzaldehyde, in $H_2$hmb o-vanillin is employed as the aldehyde component. Among other compounds, the authors report the synthesis of a 1D framework when Cu(II) acetate and solvothermal conditions are used along with the secondary linker 4,4'-bipyridine (bipy). The resulting compound, $[Cu_2(hmb)_2(bipy)]\cdot nH_2O\cdot nDMF$ (**9**) contains dicopper $Cu_2(hmb)_2$ units which are linked to each other via bipy molecules, forming a 1D hacksaw chain (Figure 8). Regarding its properties, **9** was investigated for its homogeneous activity towards the oxidation of primary and secondary alcohols to aldehydes and ketones: cyclohexanol, benzyl alcohol and 1-phenyl ethanol were tested as substrates (Scheme 6). The reaction also involves the use of microwave irradiation, aqueous *tert*-Butyl hydroperoxide (TBHP) as oxidizing agent and 0.2 mol% of **9** under 60$^o$C and solvent-free medium. Corresponding products were afforded at moderate to excellent (49-90%) yields, much higher to the respective yields afforded when Cu(II) acetate is used as the catalyst.

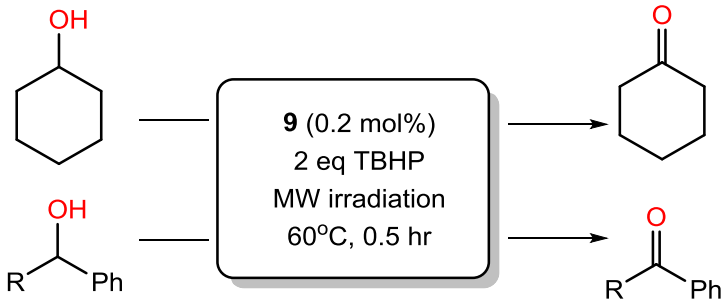


**Scheme 6.** Oxidation of alcohols to ketones catalyzed by **8**.

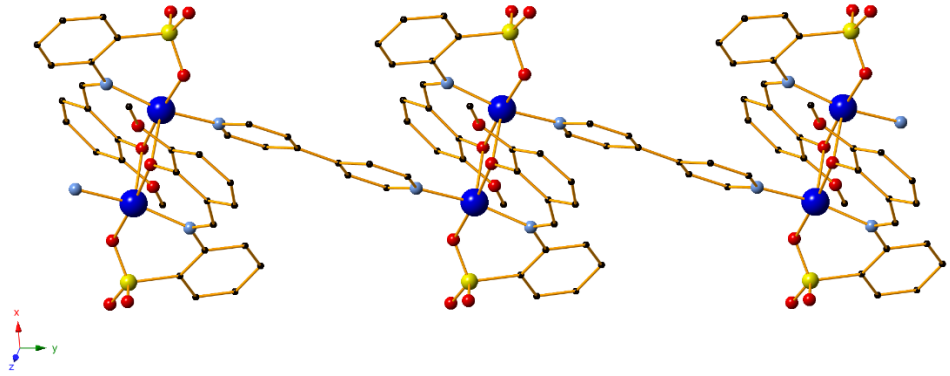

**Figure 8**. The 1D hacksaw chain in **9**. H-atoms and solvent molecules have been removed for clarity. Colour code Cu (blue), C (black), N (light blue), O (red), S (yellow).

Furthermore, a report surfaced in 2016 in which Zhang and co-authors[72] utilize amino acid Schiff base ligands to generate Cu(II) CPs with catalytic properties in the selective oxidation of sulfides to sulfoxides (Scheme 7). More specifically, the reported ligands are derived from the condensation of pyridinecarboxaldehyde analogues and an enantiopure amino acid (L-aspartic acid or L-valine), providing a targeted synthesis of chiral CPs. Treatment of these ligands with Cu(II) acetate in dioxane/water enabled for the formation of the polymeric compounds [Cu(2L-asp)($H_2O$)]·3.5$H_2O$ (**10**) and [Cu(3L-val)(OAc)($H_2O$)]·2$H_2O$ (**11**), where 2L-$H_2$asp = N-(2-pyridylmethyl)-L-aspartic acid and 3L-val = N-(3-pyridylmethyl)-L-valine. Both compounds form a 1D homochiral helical chain in which the metal centers are penta-coordinated ({$N_2O_3$} coordination environment) and possess a square pyramidal geometry (Figure 9). However, there are some differences in the helical motifs of the two frameworks due to the ligand selection: each Cu(II) center in **10** is coordinated to two carboxylate groups from L-aspartic acid, while in **11** each metal center is coordinated to one O atom of L-valine and one O atom of an acetate group. Furthermore, **10** shows a larger helical pitch compared to **11** due to the different substitution of the pyridyl group in each ligand. Out of the two compounds, **11** exhibited the most encouraging heterogeneous catalytic performance (47-99% yields) in the sulfoxidation reaction for a variety of substrates. Furthermore, it achieved very high selectivities for the sulfoxides, avoiding over oxidation to sulfones. However, the catalyst was not successful in providing high asymmetric induction (approximately 20% ee).

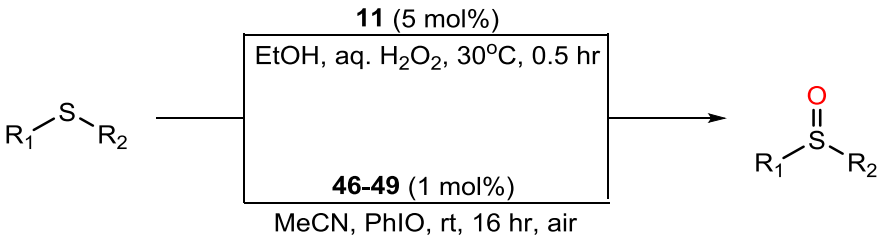


**Scheme 7.** 1D CP-catalyzed selective oxidation of sulfides to sulfoxides.

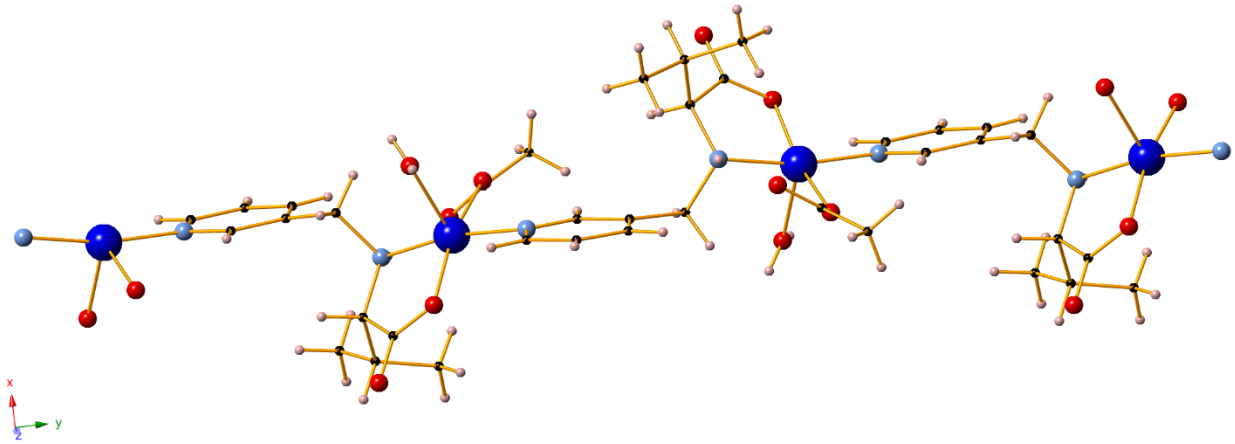

**Figure 9**. The 1D homochiral helical chain in **11**. Solvent molecules have been removed for clarity. Colour code Cu (blue), C (black), N (light blue), O (red), H (light pink).

Another strategy that has been employed in the field of catalyst development involving Schiff base ligands is the design of ligand systems towards coordination compounds which mimic the environment of known metalloproteins. A recent study by Mandal and others[73] utilizes this strategy to emulate the behavior of catechol oxidase, a dicopper enzyme which catalyzes the oxidation of catechols to ortho-quinones (Scheme 8). Each of the Cu(II) centers in the enzyme contains three nitrogen atoms from histidine molecules and an oxygen atom deriving from a bridging hydroxide molecule. The authors introduce the Schiff base ligand 4-ethyl-2,6-bis((E)-((3-morpholinopropyl)imino)methyl)phenol (Hbmmp), which is designed based on the coordination environment observed in the enzyme. During the synthesis of the compound, sodium azide is added to assist in the formation of the desired bridging and coordination environment. The resulting compound, $[Cu_2(bmmp)(N_3)_3]$ (**12**), is a 1D dicopper CP with pentacoordinated Cu(II) centers and a motif similar to catechol oxidase (Figure 10). UV-Vis studies for the oxidation of

3,5-di-tert-butylcatechol using **12** (1% M based on the catechol amount) were then performed. The resulting spectra in MeCN or DMF showed a peak at ca. 400 nm, characteristic of the corresponding o-quinone. Moreover, the turnover values for the catalyst are comparable to those of previously reported dicopper compounds with catecholase activity.

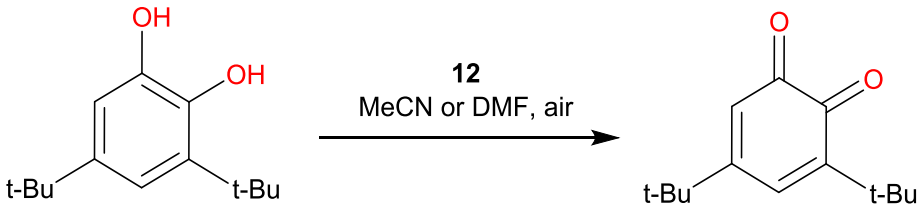


**Scheme 8.** Oxidation of 3,5-di-tert-butylcatechol to the respective quinone.

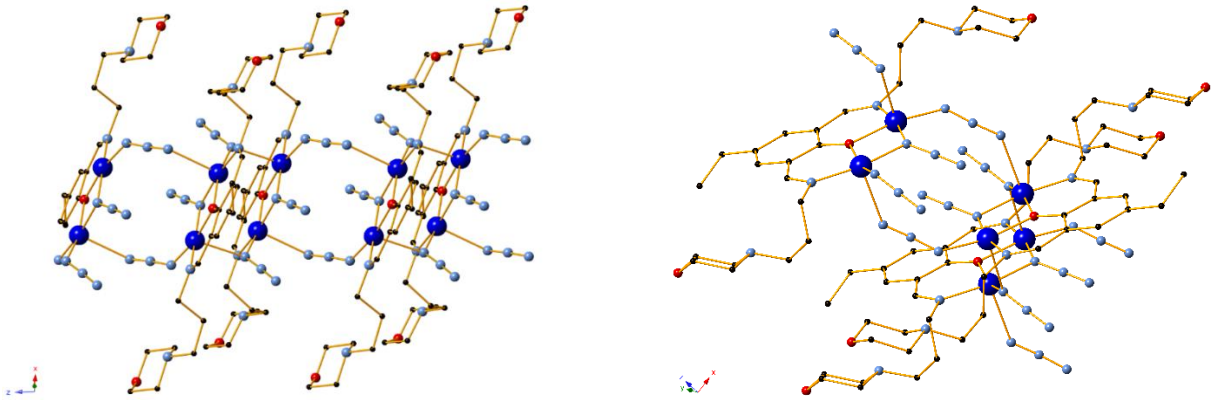

**Figure 10.** Part of the 1D framework in **12** from multiple (left, right) views. H-atoms have been removed to enhance clarity. Colour code Cu (blue), C (black), N (light blue), O (red).

The use of 1D CPs as catalysts, however, is not limited to oxidation reactions only. In a recent study by Wani[74] and co-workers, a series of novel one-dimensional polymeric compounds with transition metals (Zn, Cd, and Co) is tested for their catalytic efficiency in the transesterification reaction. In this transformation, synthesis of esters is achieved as the organic component of the alkoxy group of a different starting ester is exchanged with the organic group of an alcohol. Two different organic linkers, 2,3,5,6-tetrakis(2-pyridyl)pyrazine (tppz) and 3-(carboxymethyl-amino)-4-chlorobenzoic acid ($H_3$ccb) are used for the synthesis of CPs, providing multiple potential coordination sites to the metal centers. The resulting isostructural compounds

comprise of M(tppz) units linked by Hccb ligands with deprotonated carboxyl groups, which provide the dimensionality to the framework. This accounts for the formation of a 1D zig-zag chain where each metal center is penta-coordinated in a square pyramidal geometry (Figure 11). Out of the three CPs reported, the zinc analogue, [Zn(tppz)(Hccb)]·DMF·$H_2O$ (**13**), proved to be the most active catalyst in the transesterification reactions (Scheme 9). Very good yields were achieved when these reactions proceeded in DMSO, under 80°C and within 4 to 16 hrs, when 2 mol% of **13** was used. The catalyst may also be reused for at least four cycles without any loss in yield. As **13** has a superior activity compared to Zn(II) salts, the authors propose that this may be attributed to the unsaturated penta-coordinated Zn(II) center, which provide a free site for substrate binding.

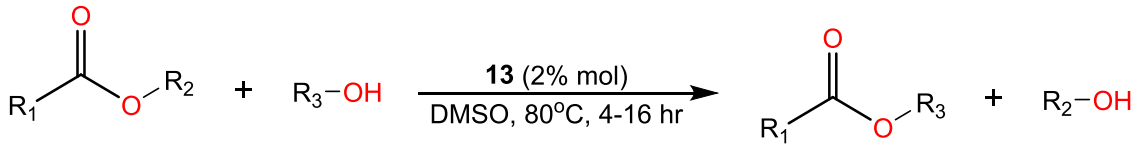


**Scheme 9.** Transesterification reaction as catalyzed by **13**.

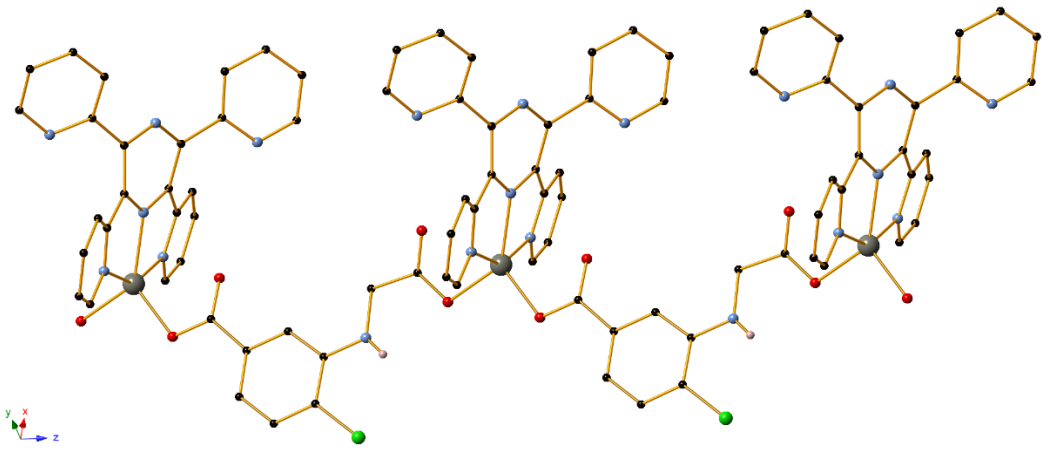

**Figure 11.** The 1D zig-zag chain in **13**. Solvent molecules and H-atoms have been removed for clarity. Colour code Zn (grey), C (black), N (light blue), O (red), Cl (green).

In 2016 Hussain and others[75] introduced a series of 1D Cu(II) CPs with catalytic potential in the transesterification of the biologically interesting phosphate ester 2-hydroxypropyl-*p*-nitrophenylphosphate (HPNP). These Cu(II) compounds were constructed using the imine-based ligands bis(2-hydroxybenzylidene)pyridine-2,6-dicarbohydrazide and bis(pyridin-2-

ylmethylene)pyridine-2,6-dicarbohydrazide ($H_4$hpd and $H_2$ppd respectively). As the study investigates the effect of the different coordination environment in the catalytic performance, the coordinating nitrate and chlorine anions were also employed to modify the environment of the metal center. This resulted to the CPs formulated as $[Cu_3(hpd)(NO_3)_2(DMF)(H_2O)]\cdot 3(DMF)$ (**14**), $[Cu_3(hpd)(Cl)_2(DMF)_2]$ (**15**) and $[Cu_3(ppd)(NO_3)_4(H_2O)_4]$ (**16**). These modifications result to different 1D frameworks in each compound: in **14**, the polymeric architecture is formed through bridging of phenolic oxygen atoms from ligand molecules, constructing a 1D sheet. In **15** and **16**, bridging occurs through the coordinating chlorine and nitrate anions respectively, resulting in a 1D zig-zag (**15**) or chain (**16**) coordination polymer (Figures 12-14). Interestingly, **14** shows very high catalytic activity in the transesterification reaction, while **16** has much inferior performance and the catalytic effect of **15** is negligible. The authors attribute these findings to the architecture and coordination environment of the CPs: it is proposed that the reaction is promoted by the presence of coordinated water molecules, which are then deprotonated under the high pH to generate nucleophile sites; thus, explaining the very low activity of **15**. Furthermore, it is suggested that the 1D sheet framework in **14** promotes a cooperative effect between the metal centers, which are found in a distance of approximately 3 Å, greatly enhancing the catalytic activity. In contrast, the bridged Cu centers in **16** are in a distance of 6.85 Å due to the formation of the zig-zag framework.

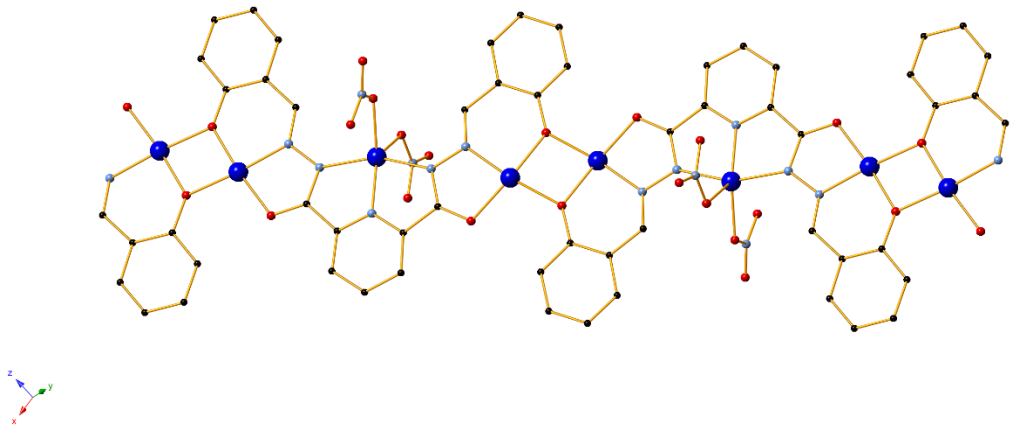

**Figure 12.** The 1D sheet formation in **14**. Lattice solvent molecules and H-atoms have been removed for clarity. Colour code Cu (blue), C (black), N (light blue), O (red).

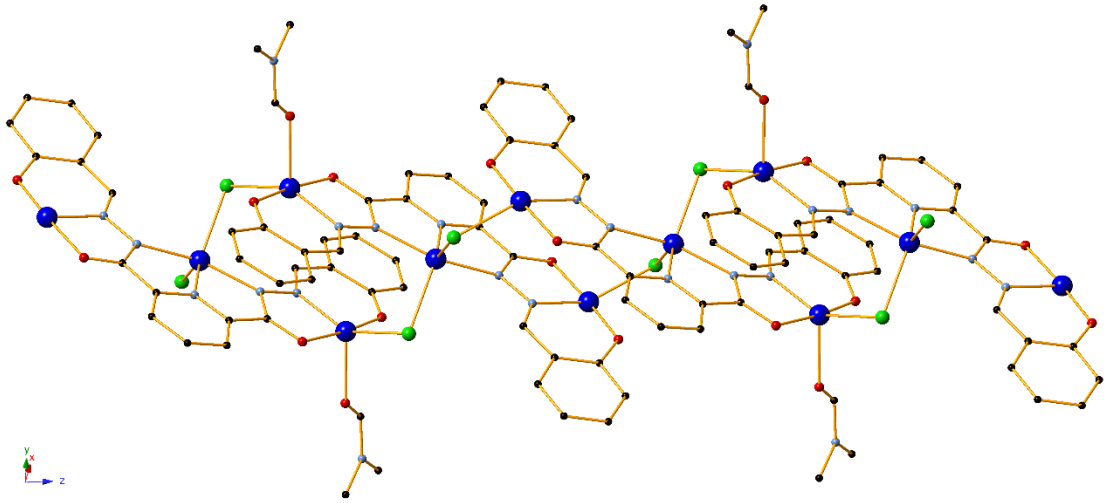

**Figure 13.** The 1D zig-zag architecture in **15**. Lattice solvent molecules and H-atoms have been removed for clarity. Colour code Cu (blue), C (black), N (light blue), O (red), Cl (green).

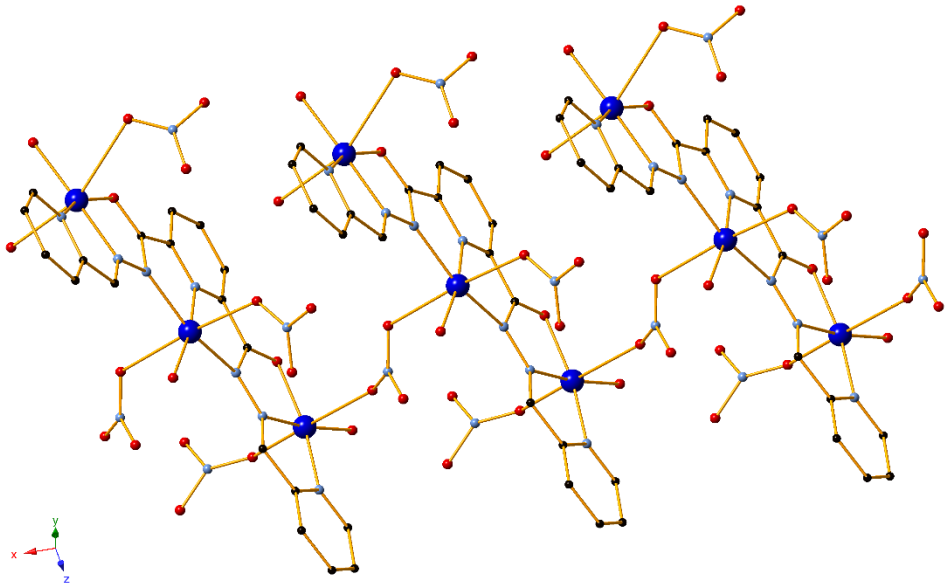

**Figure 14.** Formation of a 1D chain in **16**. Lattice solvent molecules and H-atoms have been removed for clarity. Colour code Cu (blue), C (black), N (light blue), O (red).

Another report of a 1D CP with interesting activity surfaced in 2016, when Zhu and co-authors[76] presented a Cu(I) coordination compound with multifunctional heterogeneous catalytic performance. In this case, an imidazole-based ligand is employed (dfbi = 1,1'-(9,9-dimethyl-9H-fluorene-2,7-diyl)bis(1H-imidazole)) along with Cu(II) bromide; *in situ* reduction of Cu(II) to

Cu(I) then occurs to afford a structure with two crystallographically independent Cu(I) centers: the first features in the formation of [$CuL_2$] units in an almost linear fashion, while the second center participates in the formation of [$CuBr_2$]$^-$ outer hanging species. The resulting CP, [Cu(dfbi)($CuBr_2$)], (**17**) presents a 1D zig-zag architecture as featured in Figure 15. One of the reactions that **17** catalyzed was the acetylation of substituted phenols to produce the corresponding acetate esters. In the proposed work scheme, the reaction takes place in $CH_2Cl_2$ for 2 to 15 hours under room temperature conditions and in the presence of 5 mol% of **17**. Resulting acetates are afforded in excellent conversions of 99%, while the catalyst is reusable for at least five runs with no losses in performance. Interestingly, the authors suggest that the Lewis acid nature of the [$CuBr_2$]$^-$ moiety is the main reason for the excellent activity of **17** as it allows for easier access for the nucleophilic substrates. Furthermore, the linear geometry of the Cu(I) centers could further facilitate the activity, providing plenty of room for additional substrate binding to the metal sites.

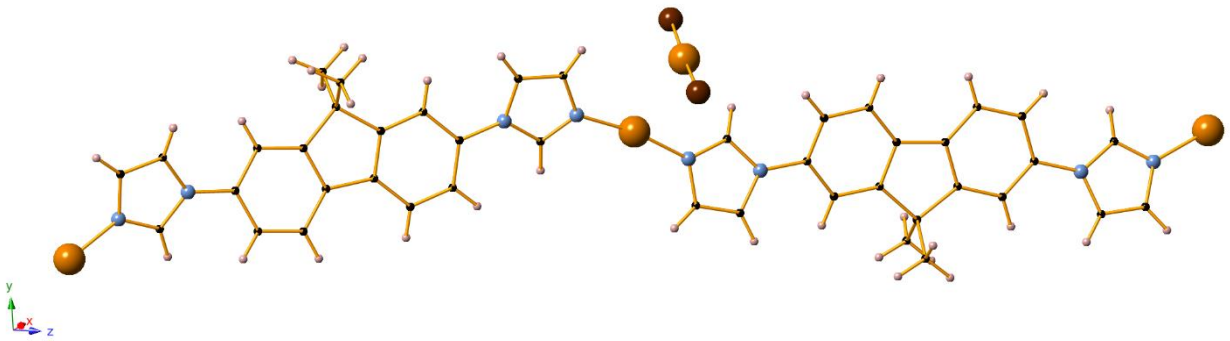

**Figure 15.** The 1D zig-zag chain in **17**. Colour code Cu (light orange), C (black), N (light blue), Br (brown), H (light pink).

In another relevant organic transformation, the versatility of epoxides as building blocks in synthesis has been particularly used in styrene oxide alcoholysis reactions in order to produce β-amino alcochols. These ring-opening reactions typically require the presence of a catalyst to proceed efficiently and at non-high temperatures. In 2013 a lanthanide-based 1D coordination polymer introduced by Vilela and co-authors[77] was found to be a highly active heterogeneous catalyst in this reaction. The compound was synthesized using $LaCl_3 \cdot 7H_2O$ and the tripodal ligand (benzene-1,3,5-triyltris(methylene))triphosphonic acid ($H_6$bmt) under aqueous conditions. The resulting structure, [La($H_4$bmt)($H_5$bmt)($H_2O$)$_2$]$\cdot 3H_2O$ (**18**) forms a 1D zig-zag architecture (Figure

16) in which each lanthanum center is coordinated to four symmetry-related ligand molecules which are partially deprotonated, thus possessing a square antiprismatic environment. The compound was then tested in various concentrations (as low as 3.3 g $L^{-1}$) for its catalytic activity in the methanolysis of styrene oxide under atmospheric air, in 55$^{o}$C and with a reaction time of 60 minutes (Scheme 10). Under these conditions, 2-methoxy-2-phenylethanol was afforded at quantitative amounts; the catalyst was additionally reused for four cycles, retaining excellent yields above 90%. To provide more insight in the performance of **18**, the catalytic activity of the metal salt ($LaCl_3 \cdot 7H_2O$) as well as the $H_6$bmt ligand was investigated. While the former only showed conversion of 4%, the latter worked excellently as a catalyst to provide 100% yield after 1 hr of reaction time. It is therefore proposed that the active sites of **18** are of Brönsted type, which is attributed to the ligand component and promotes the reaction. Despite the excellent activity of $H_6$bmt, **18** is still preferred as a catalyst due to its heterogeneous nature and its easier handling.

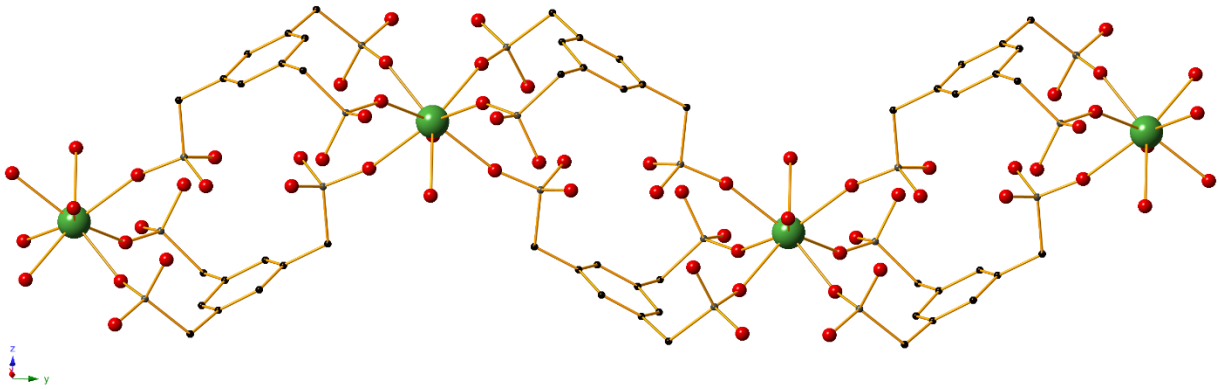

**Figure 16.** Part of the 1D framework in **18**. Lattice solvent molecules and H-atoms have been removed for clarity. Colour code La (light green), C (black), O (red), P (dark grey).

Another one-dimensional lanthanum(III) coordination polymer was proposed as a catalyst in this reaction in 2015 by Mendes and co-workers[78]. Once again, a tripodal polyphosphonate ligand, nitrilotris(methylenephosphonic acid) ($H_6$nmp), was employed. Addition of $La_2O_3$ resulted to the formation of a dilanthanum coordination polymer, $[La_2(H_3nmp)_2(H_2O)_4] \cdot 4.5H_2O$ (**19**), which propagates to one dimension through a zig-zag architecture (Figure 17). **19** was identified as a suitable heterogeneous catalyst in the alcoholysis of styrene oxide with either methanol or ethanol (Scheme 10), with excellent yields up to 99% and at relatively low concentrations (20 g $L^{-}$

[1]) of the catalyst. The compound can then be reused for at least three cycles without any noticeable losses of performance. Typical conditions for the reaction involve stirring at 35°C for up to 6 hrs. It is worth noting that the activity of this 1D CP outperforms several 3D MOFs which have been tested for this reaction.

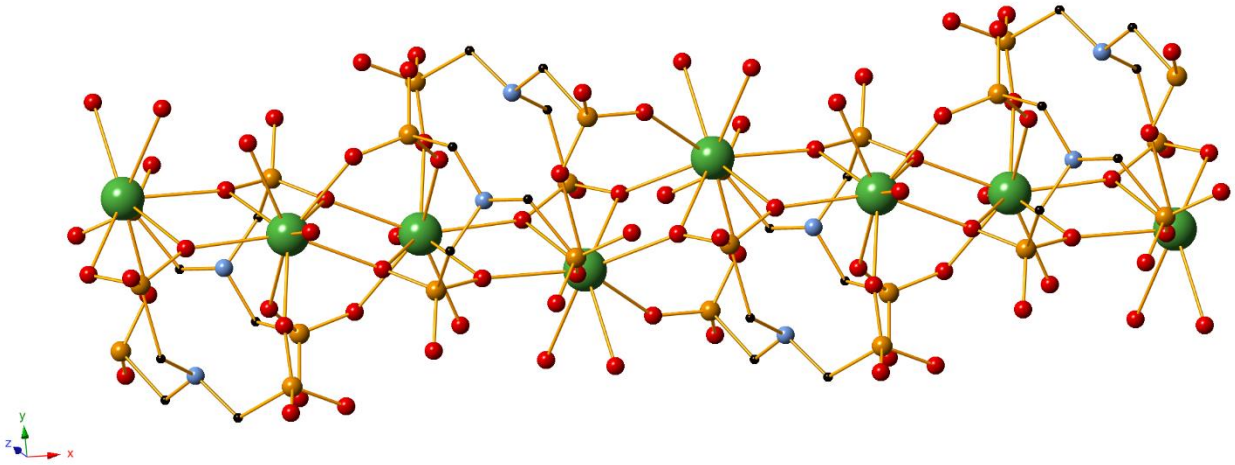

**Figure 17.** Part of the 1D framework in **19**. Lattice solvent molecules and H-atoms have been removed for clarity. Colour code La (light green), C (black), N (light blue), O (red), P (orange).

In addition, the multifunctional Cu(I) CP **17** has also been successfully tested in this transformation. The reaction conditions were optimized when only 2 mol% catalyst was used, under 50°C temperature and in methanol, stirred for 7-24 hours (Scheme 10). Good to excellent (67-97%) yields were obtained for various aromatic and non-aromatic substrates. **17** can be then reused for up to seven catalytic cycles with only slight losses in activity.

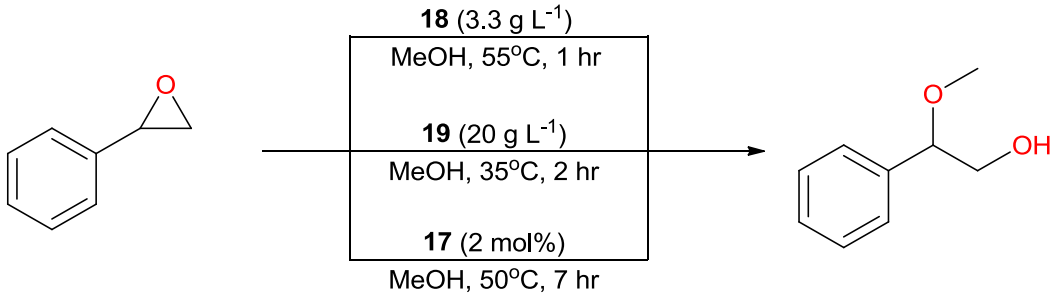


**Scheme 10.** 1D CP-catalyzed styrene oxide alcoholysis.

Although 1D CPs have been mainly used as catalysts in already known organic transformations, a recent study by our group highlights their potential in a new pathway towards the synthesis of substituted 1,4-dihydropyridines (1,4-DHPs)[79]. 1,4-DHPs and their derivatives are an important class of biologically active organic compounds, due to their activity as calcium channel blockers[80]. Several DHP analogues such as amlodipine[81], nifedipine[82], felodipine[83] have been used extensively in pharmacology as antidepressants[84], antitumoral[85,86], antianxiety[87] and anti-inflammatory agents[88,89]. The known methodologies for the synthesis of 1,4-DHPs include Hantzsch[90], multicomponent[91], cycloaddition[92] or C–C coupling reactions[93], using a large number of proposed catalysts. However, these typically exhibit certain drawbacks (e.g, high reagent cost, difficult conditions, tedious work up). Our study introduces a Cu(II) CP, formulated as $[Cu(bbmb)_2(MeCN)_2]\cdot 2(ClO_4)\cdot 2MeCN$ (**20**) and constructed with 1,2-bis((1H-benzo[d][1,2,3]triazol-1-yl)methyl)benzene as bbmb. The structure of **20** extends to one dimension along the a axis to form a 1D framework with small voids (Figure 18). Each Cu(II) is coordinated to six nitrogen atoms to possess a octahedral geometry in which the axial positions are occupied by the acetonitrile nitrogen atoms. **20** was found to catalyze a previously unknown chemical transformation between symmetrical electron-rich aldrazines and alkyl propiolates to generate 5-aryl-1-(benzylideneamino) 1,4-dihydropyridines in a one-pot synthesis and under mild conditions (Scheme 11) in good isolated yields up to 67%. It is worth noting that none of the Cu(II) salts catalyzed the reaction. Furthermore, characterization and fine tuning of **20** revealed details on the possible mechanism: a Cu(I) material was recovered after the end of the reaction, and cyclic voltammetry of **20** revealed a reversible reduction process, assigned to the $[Cu^{II}]\leftrightarrow[Cu^{I}]$ couple. Additionally, a 2D CP was constructed using Cu(II) nitrate and bbmb, giving no conversion in the reaction; the 1D Zn(II) isostructural analogue of **20** was also synthesized, but showed no catalytic activity. This data enabled for a clearer proposed mechanism for this unknown transformation: this initially involves the formation of a Cu(II)/azine intermediate, followed by a single electron transfer from the azine to the intermediate to initially generate a Cu(I) active species. A Cu(I) acetylide (propiolate) intermediate is then formed, undergoing a cyclization process followed by a [4+2] to give the resulting 1,4-DHP.

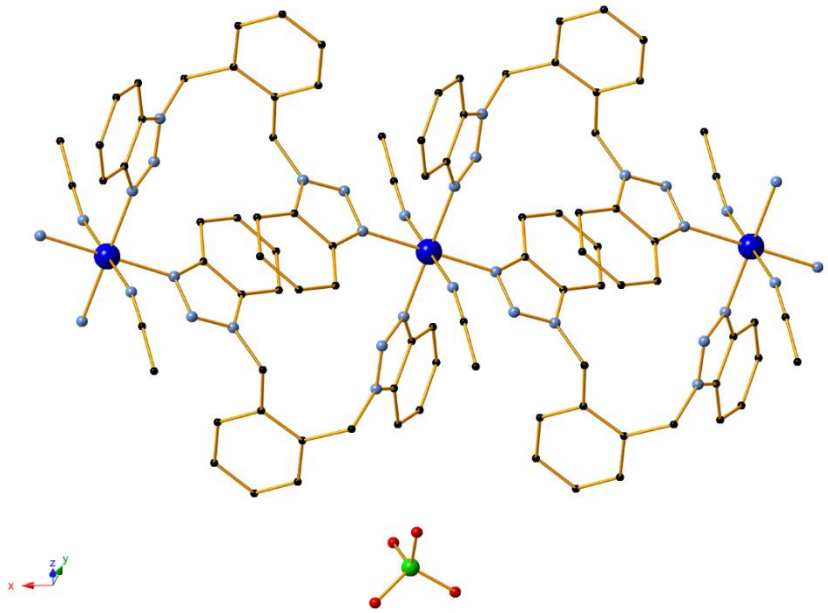

**Figure 18.** Part of the 1D framework in **20**. Lattice solvent molecules and H-atoms have been removed for clarity. Colour code Cu (blue), C (black), N (light blue), O (red), Cl (green).

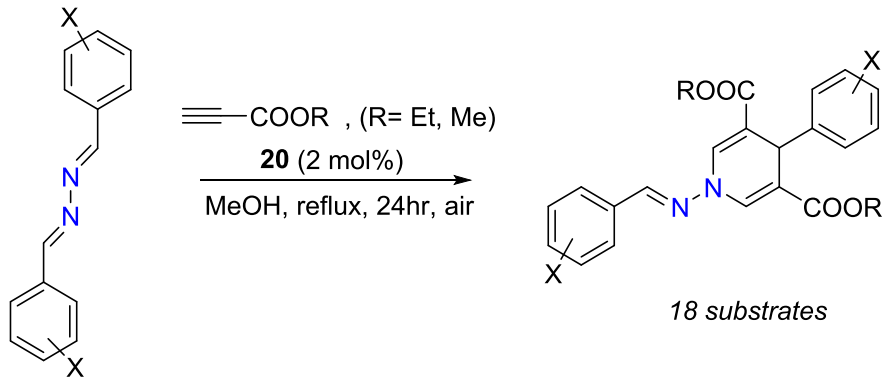


**Scheme 11.** Formation of 1,4-DHPs from aldrazines and alkyl propiolates as catalyzed by **20**.

This type of Cu(II) CPs were further studied by our group as we sought to explore their potential into other chemical transformations. Recently, we investigated their effect in the multicomponent $A^3$ coupling reaction of an aldehyde, an amine and an alkyne[94]. This reaction yields propargylamines, which are important synthetic blocks towards nitrogen-containing biologically active compounds[95,96]. This reaction was specifically selected as its commonly suggested mechanism (which involves the reduction of the metal source and the formation of a metal-acetylide intermediate) resembled the proposed catalytic function of our system and would

provide us with an excellent opportunity for fine tuning. We therefore introduced a series of Cu(II) compounds in order to investigate the role of dimensionality and coordination environment in the catalytic system. This enabled us to identify the optimal 1D catalyst, $[Cu(bbmb)_2(CF_3SO_3)_2]$ (**21**), which contains an isostructural (Figure 19) framework to **20** and avoids any issues that would inhibit its catalytic performance. As a result, good to excellent yields (57-100%) for a range of propargylamines (with much superior efficiency compared to Cu(II) salts) were obtained when the reaction was carried out in 2-propanol, heated at 90°C and using 2 mol% of **21** (Scheme 12). The results are also consistent with the commonly suggested mechanism.

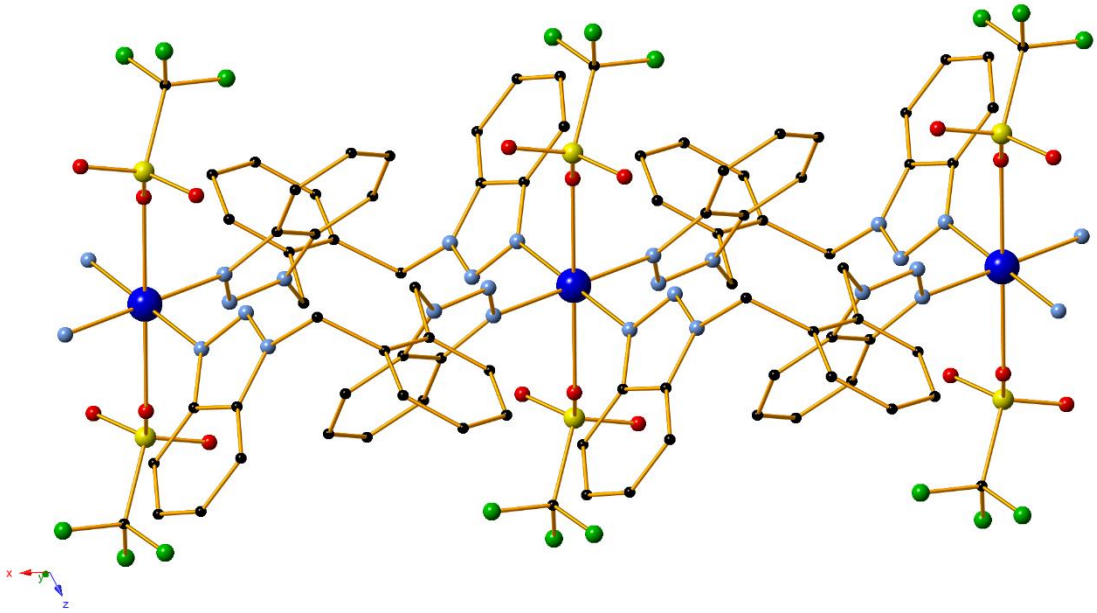

**Figure 19.** Part of the 1D framework in **20**. H-atoms have been removed for clarity. Colour code Cu (blue), C (black), F (green), N (light blue), O (red), S (yellow).

While **21** is the first Cu(II) 1D CP to be employed in the $A^3$ coupling, in 2012 Zhao and co-workers[97] introduced a Ag(I) coordination polymer as a potential catalyst in this reaction. Formulated as $[Ag(bdob)(NO_3)]$ (**22**), it is synthesized using 1,4-bis(4,5-dihydro-2-oxazolyl)benzene (bdob) and forms a one-dimensional zig-zag framework. Each Ag(I) center is coordinated to the ligand only through nitrogen atoms possessing a trigonal coordination geometry. As the compound was insoluble in organic solvents, it was tested as a heterogeneous catalyst in the $A^3$ coupling of aldehydes, secondary amines and phenylacetylene. The proposed conditions for the reaction included the use of 1.9 mol% of **22** in chloroform and under room temperature (Scheme 12). This provided moderate to excellent conversions which ranged from 32 to 96%, with

the aliphatic aldehyde substrates displaying the highest reactivity. Furthermore, the catalyst was reused for four cycles without any significant loss of conversion.

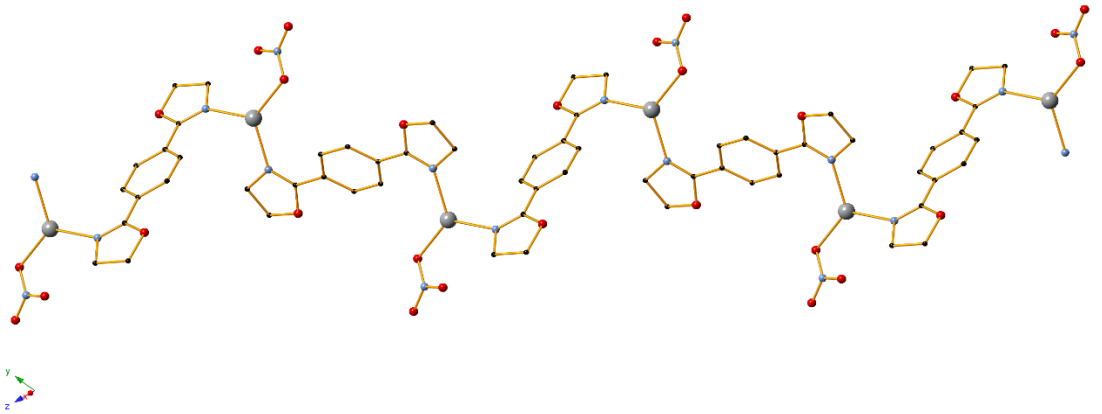

**Figure 20.** The 1D zig-zag framework in **22**. H-atoms have been removed for clarity. Colour code Ag (grey), C (black), N (light blue), O (red).

The $A^3$ reaction was also one of the reactions catalyzed by the multifunctional Cu(I) CP **17** reported earlier in this review. In this case, the reaction occurs for 6 hours in room temperature, under solvent-free conditions and 5 mol% of the catalyst (Scheme 12). When aliphatic aldehydes are employed, the corresponding propargylamines are afforded in excellent yields ranging from 86 to 94%.

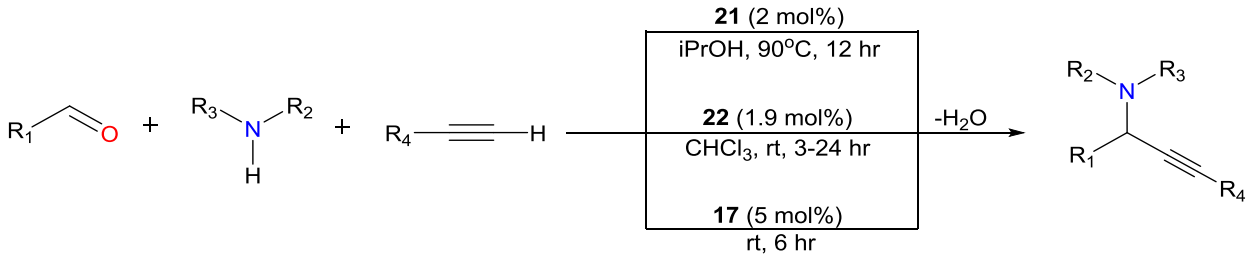


**Scheme 12.** 1D CP-catalyzed $A^3$ coupling.

More examples of 1D CPs in catalysis have also been recently identified in the nitroaldol reaction, more commonly known as the Henry reaction. This C-C coupling between a nitroalkane

and a carbonyl compound (aldehyde or ketone) provides an important route for the synthesis of β-nitroalcohols[98]; these can be then employed as starting materials towards numerous synthetic procedures. In 2015, Hazra, Karmakar and co-workers[99] reported the synthesis of a new Cu(II) compound, based on the Schiff-based ligand 2-(2-pyridylmethyleneamino)benzenesulfonic acid (pmba), which propagates though dicyanamide bridges to form a one-dimensional polymeric chain (Figure 21). This Cu(II) 1D CP, $[Cu(pmba)(\mu_{1,5}\text{-}C_2N_3)]\cdot H_2O$ (**23**) was found to be a new homogeneous catalyst for the Henry reaction of nitroethane with various aromatic and aliphatic aldehydes to produce the corresponding b-nitroalkanols with moderate to excellent yields (24-94%) and good diastereoselectivities (*syn:anti* up to 4:1). The proposed method uses environmentally friendly conditions (aqueous medium, air atmosphere) and low catalyst loadings of 1 mol% (Scheme 13). It is suggested that ligand selection may also play an important part in the catalytic activity, as the sulfonate group could assist to the proton abstraction from the nitroalkane and the protonation of the C–C coupled species.

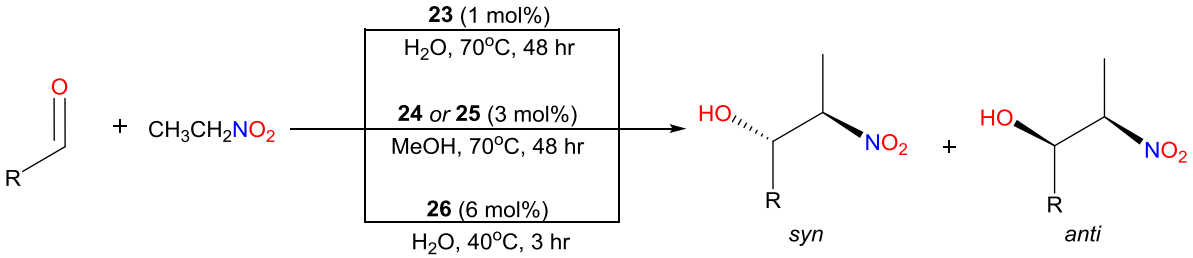


**Scheme 13.** 1D CP-catalyzed Henry reaction.

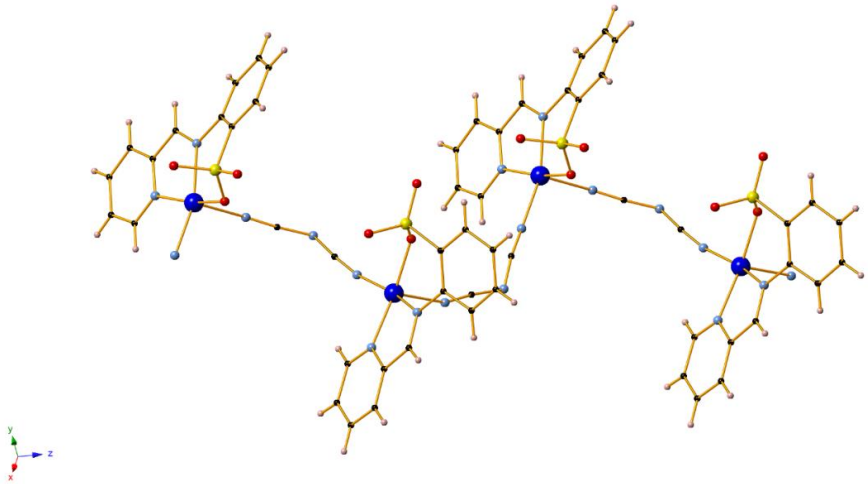

**Figure 21.** The 1D framework formed in compound **23**. Lattice solvent molecules have been removed for clarity. Colour code Cu (blue), C (black), N (light blue), O (red), S (yellow), H (light pink).

Also in 2015, the same group designed the synthesis of a number of Zn(II) coordination compounds with amidoisophthalate linkers, in an effort to further investigate the catalytic potential of CPs in the Henry reaction[100]. Employment of 5-benzamidoisophthalic acid ($H_2$bipa) as ligand led to the synthesis of the 1D CPs [Zn(bipa)($H_2O$)$_2$] (**24**) and [Zn(bipa)($H_2O$)$_2$]·2$H_2O$ (**25**). While in both CPs the metal centers contain the same tetrahedral {$O_4$} coordination environment, the carboxylate groups coordinate in anti (**24**) or syn (**25**) fashion in each case, which leads to a respective helical- or zigzag-type polymeric chain (Figures 22 and 23). From a catalytic point of view, these amidoisophthalate-based CPs have low solubility and act as efficient heterogeneous catalysts in the Henry reaction. Under the optimal reactions conditions as seen in Scheme 13, compound **24** showed the best catalytic activity for a range of aromatic and aliphatic aldehydes with yields ranging from 37 to 97% and up to 6:1 diastereoselectivity (*syn:anti*). In terms of reusability, the catalyst was recycled for six consecutive experiments, retaining its activity almost the same.

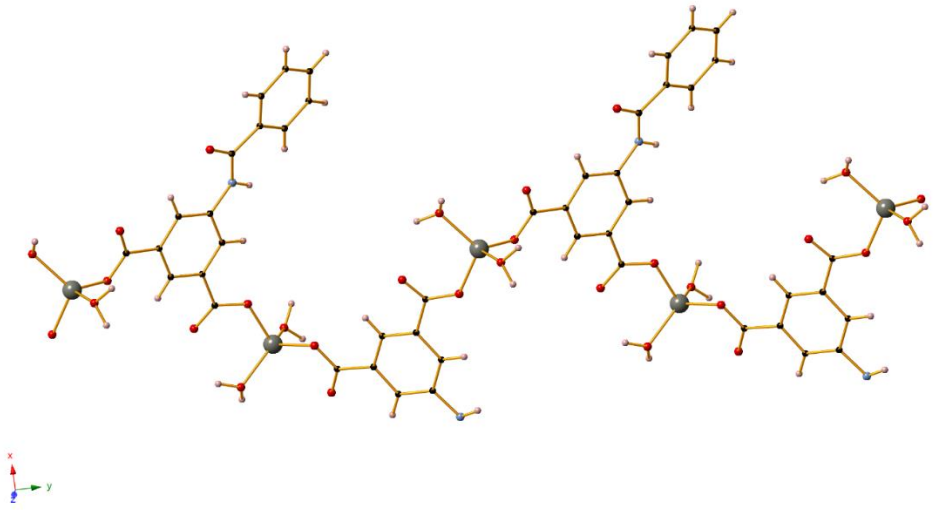

**Figure 22.** The 1D helical chain in **24**. Colour code Zn (grey), C (black), N (light blue), O (red), H (light pink).

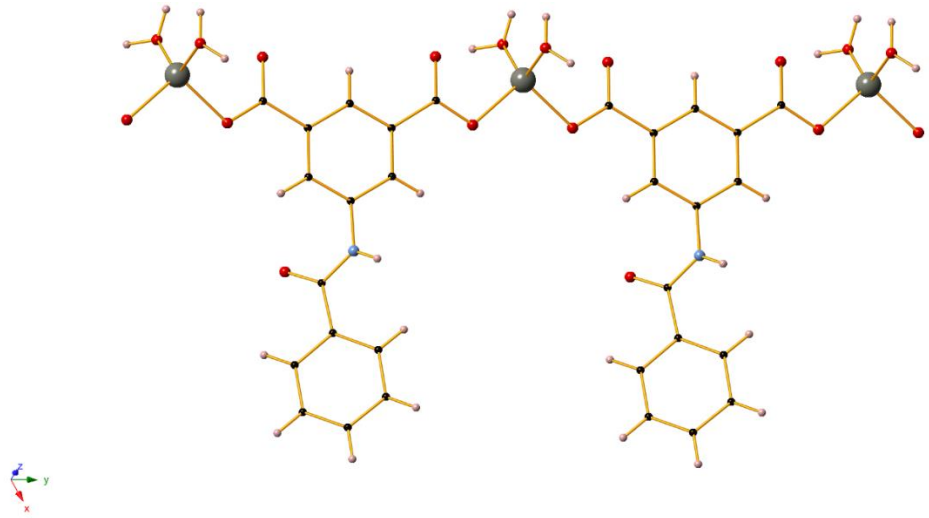

**Figure 23.** The 1D zig-zag chain in **25**. Lattice solvent molecules have been removed for clarity. Colour code Zn (grey), C (black), N (light blue), O (red), H (light pink).

Very recently, another Zn(II) coordination polymer with catalytic activity in this reaction was introduced by Martins and others[101]. The ligand used was 5-(2-(4,4-dimethyl-2,6-dioxocyclohexylidene)hydrazinyl)isophthalic acid ($H_3$dhia); it contains two carboxylic groups in order to generate compounds with dimensionality as well as to introduce higher solubility in aqueous medium, towards environmentally friendly catalysis. Indeed, in the resulting compound [Zn(Hdhia)($H_2O$)$_2$]·$H_2O$ (**26**) one of the carboxylic groups links two Zn(II) centers in a bridging bidentate mode and the remaining one ligates a third metal center in a monodentate fashion, enabling the structure to propagate to one dimension (Figure 24). **26** was then successfully applied as a green homogeneous catalyst for the diastereoselective Henry reaction in water with good yields (up to 86%) and diastereoselectivities (*syn:anti* up to 3:1) for both aromatic and aliphatic aldehydes (Scheme 13).

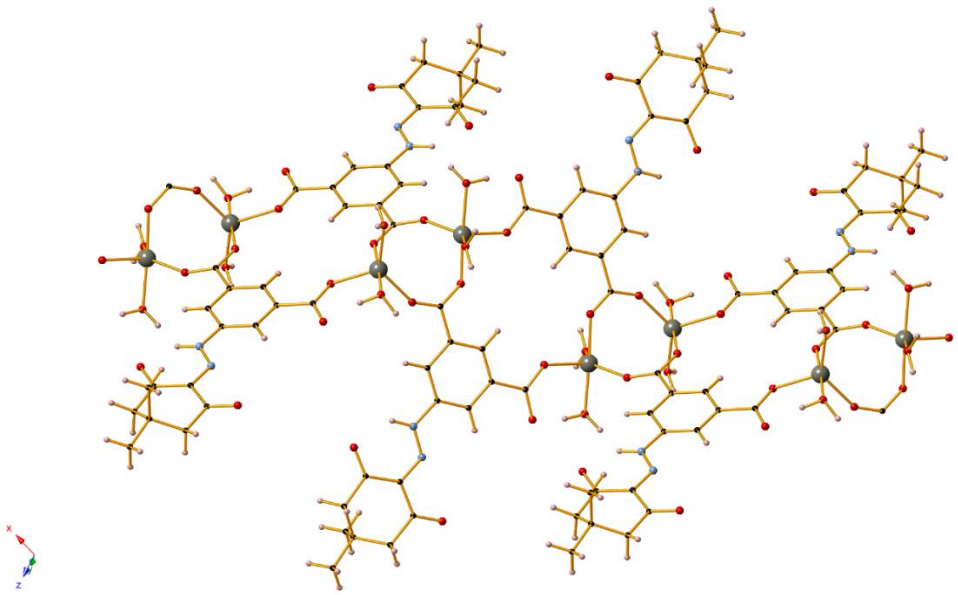

**Figure 24.** Part of the 1D framework in **26**. Lattice solvent molecules have been removed for clarity. Colour code Zn (grey), C (black), N (light blue), O (red), H (light pink).

The Knoevenagel reaction[102] is another chemical transformation in which the catalytic potential of 1D CPs has been studied recently. This C-C bond formation reaction affords α,β-unsaturated compounds from the condensation of a carbonyl compound and an active hydrogen compound, which is then deprotonated by the catalyst. Recently, Karmakar and co-workers[103] reported the synthesis of several Zn(II) coordination polymers using 5-acetamidoisophthalic acid ($H_2$aipa) as the primary linker. Interestingly, the topology of the resulting structures was found to be dependent on the solvent used in each case. Experiments under the presence of NMF (N-methylformamide) led to the synthesis of the 1D zig-zag CP, [Zn(aipa)($H_2O$)$_2$]·NMF (**27**) (Figure 25). This compound was found to have the best performance as a heterogeneous catalyst for the Knoevenagel condensation reaction (Scheme 14) with various aldehydes and malononitrile used to produce the corresponding benzylidenemalononitriles. Moreover, the catalyst was found to be recyclable without any considerable loss of activity. The suggested mechanism by the authors involves a synergistic effect by the Lewis acid (Zn centers) and basic (carboxylate-O or amide-O) sites, highlighting the importance of the metal and ligand selection when choosing the synthetic and catalytic systems.

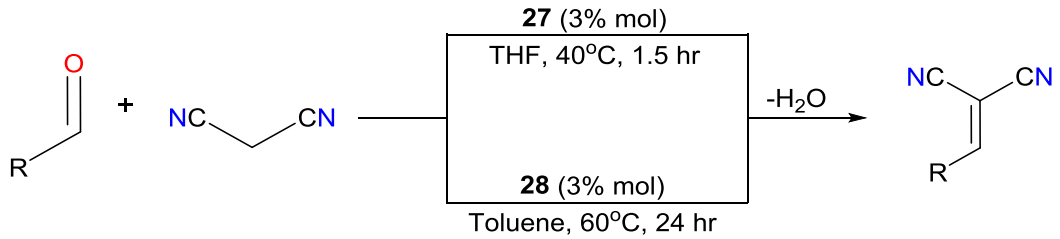


**Scheme 14.** 1D CP-catalyzed Knoevenagel reaction.

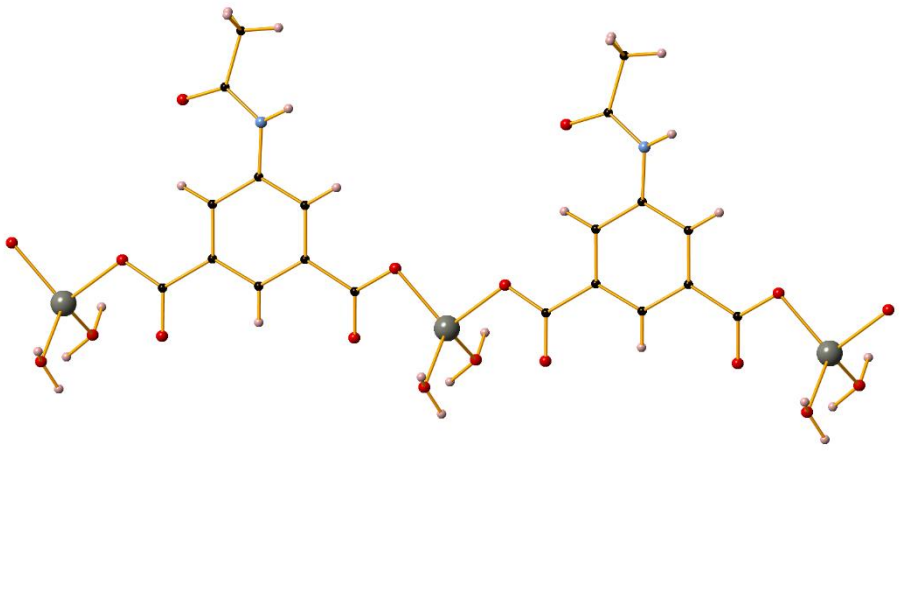

**Figure 25.** Part of the 1D zig-zag framework in **27**. Lattice solvent molecules have been removed for clarity. Colour code Zn (grey), C (black), N (light blue), O (red), H (light pink).

In 2016, Larrea et al[104] employed two different organic linkers, 1,1,2,2-tetraacetylethane ($H_2$tae) and bipy to construct a one-dimensional zig-zag Cu(II) coordination polymer, [Cu($NO_3$)($H_2O$)(Htae)(bipy)] (**28**). The compound extends to one dimension through the formation of Cu−bipy bridging chains, while the second linker is partially deprotonated and acts as a simple chelating ligand. As a result, atoms from the two linkers occupy the equatorial positions of the Cu(II) center; solvent and anion molecules are also coordinated to complete its octahedral geometry. These molecules were then removed from the structure with a thermal treatment to produce unsaturated copper centers, giving rise to the 1D framework depicted in Figure 26. The

material was then used successfully as a heterogeneous Lewis acid catalyst in the Knoevenagel condensation reaction (Scheme 14), although the catalyst is poisoned after four cycles. A typical reaction for this system takes place in toluene, under 60$^{o}$C and 3 mol% of the catalyst.

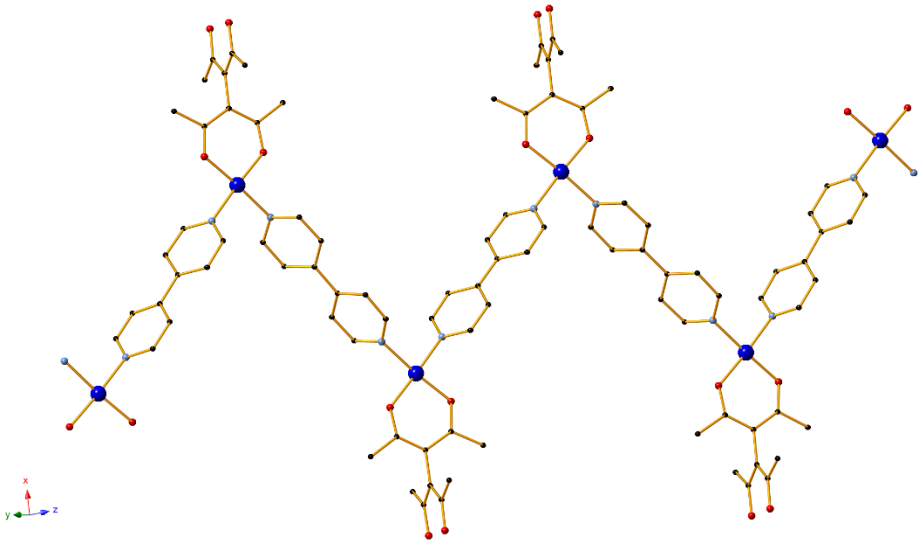

**Figure 26.** Part of the 1D architecture of **28**. H-atoms, solvent and anion molecules have been removed for clarity. Colour code Cu (blue), C (black), N (light blue), O (red).

In recent years CPs have also been employed as catalysts in the cyanosilylation of carbonyl compounds. The resulting cyanohydrins are versatile components in synthetic chemistry and act as intermediates in the preparation of compounds such as β-amino alcohols or α-hydroxy aldehydes. Trimethylsilyl cyanide (TMSCN) is the most commonly used cyanide source for the formation of cyanohydrins[105,106], however the use of a catalyst is also necessary in order to activate both the substrate and the cyanide precursor. A 1D CP with relevant catalytic behavior was presented in 2016 by Pombeiro's group[107]. The authors study the coordination capabilities of a rigid dicarboxylic acid ligand, named as 3,3″-dipropoxy-[1,1′:4′,1″-terphenyl]-4,4″-dicarboxylic acid ($H_2$dtda), with metal sources of 3d elements such as Zn(II) and Cu(II). Out of the four reported compounds, the one-dimensional analogue synthesized with Zn(II) nitrate was found to have the best catalytic performance in the aforementioned reaction. The compound, formulated as [Zn(dtda)(DMF)$_2$] (**29**), features a zig-zag chain in which both oxygen atoms of each carboxylate group of the ligand molecule coordinate to a Zn(II) center, while oxygen atoms from DMF molecules occupy the axial positions of the resulting octahedron (Figure 27). **29** was then applied

as a catalyst in a protocol that involved stirring of TMSCN and the aldehyde component in dichloromethane, for 10 hours and under room temperature (Scheme 15). Remarkably, this procedure affords cyanohydrin derivatives with good to excellent (65-91%) yields and for a good range of aromatic and aliphatic substrates when only 2 mol% of **29** is used. In comparison, Zn(II) nitrate has a poor catalytic behavior in the reaction, providing only 16% yield of the product. Furthermore, **29** may be reused for at least five cycles without any loss in activity. The authors propose that the 1D zig-zag architecture of **29** provides easy access to its Zn(II) sites, which could explain the high catalytic performance.

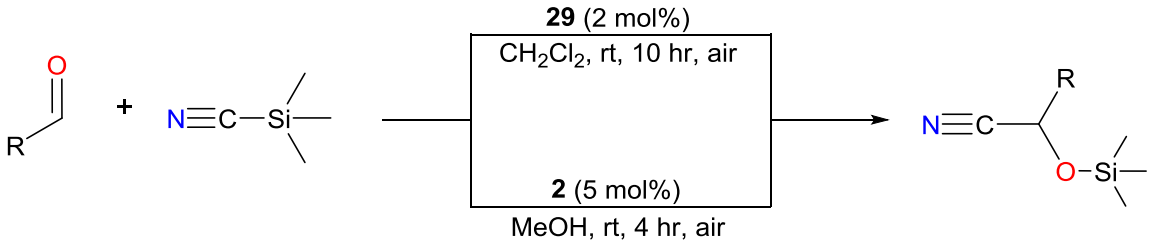


**Scheme 15.** 1D CP-catalyzed cyanosilylation of aldehydes.

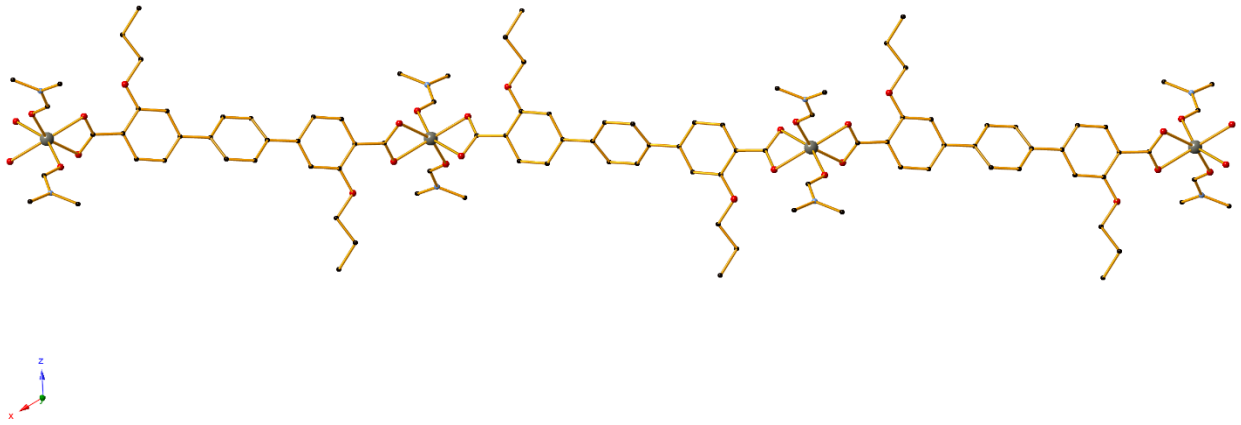

**Figure 27.** Part of the 1D framework in compound **29**. H-atoms have been removed for clarity. Colour code Zn (grey), C (black), N (light blue), O (red).

In the same year, Ma and co-workers[108] reported a series of one-dimensional Cu(II) CPs that can also catalyze this reaction. The highest conversions were achieved with the use of the already reported coordination polymer **2**, which had been previously tested in the oxidation of cyclohexane. The compound works as an excellent homogeneous catalyst as the corresponding

cyanohydrin derivatives are afforded at excellent yields which range from 86 to 99%. Optimal conditions for this reaction included the use of 5 mol% **2** and methanol as solvent, under room temperature and in 4 hours reaction time (Scheme 15). From a mechanistic point of view, the authors report the identification of several reaction intermediates by ESI-MS, which explain the effectiveness of **2**: it is proposed that the aldehyde coordinates to one of the two metal centers, displacing a water molecule. This intermediate reacts with TMSCN to form another intermediate in which a non-covalent $Si\cdots O_{aldehyde}$ bond is formed. This is followed by the nucleophilic attack of the cyanide group to the carbonyl group of the aldehyde in order to generate the resulting product, which is replaced by water in the CP to complete the catalytic cycle.

In recent years the increasing amount of industrial wastewaters has become one of the main concerns for the environment. The technique of catalytic photodegradation has emerged as an ideal method for the treatment of these wastewaters in an environmentally friendly way. Generally, semi-conductor metal compounds (e.g. oxides[109] or sulfides[110]) are most commonly used in this technique to decompose organic dyes under UV-Vis light, rendering them harmless. Due to the energy transfer between the metal centers and ligands, CPs have also been investigated recently for their potential in such methods[111]. An example of a 1D CP used for these purposes was presented in 2012 by Geng and co-workers[112]. The authors reported the synthesis of a Ag(I) compound (**30**) using a flexible bis(benzimidazole) ligand, 1,1'-(1,4-butanediyl)bis-1H-benzimidazole) (bbbi), as well as the co-linker pyridine-2,6-dicarboxylate ($H_2$pydca). The structure of **30** features $[Ag_2(pydca)_2]$ units which are bridged by bbbi molecules to form a one-dimensional helical chain (Figure 28). **30** was then tested as a catalyst in the photodegradation of the carcinogenic azo compound Methyl Orange (MO). The procedure for this was similar to the Fenton reaction, involving the use of persulfate anions to produce sulfate radicals ($SO4^{\cdot-}$), which then strongly oxidize the contaminant to destroy it; a characteristic absorbance of MO at 506 nm allowed for the monitoring of the reaction. It was found that **30** is a very active heterogeneous catalyst for the reaction, reaching a degradation efficiency of 83% after 2.5 hrs. In comparison, control experiments in absence of catalyst showed a much lower degradation percentage of 10%. In a similar strategy for the construction of the 1D architecture, Hou and co-workers[113] reported in 2013 a Co(II) coordination polymer with bbbi which extends to one dimension through the formation of an infinite chain. The compound, formulated as $[CoCl_2(bbbi)_2]\cdot$(DMF) (**31**), was

successfully used in the photodegradation of Congo Red (CR), another carcinogenic azo dye. It was found that **31** could catalyze this transformation achieving 64% degradation efficiency under room temperature and after only 75 minutes. Once again, persulfate anions were employed as the source of the oxidizer. Two more 1D CPs based on Ag or Co and the bbbi ligand were reported in 2013 by Qin[114] and co-authors, exhibiting catalytic properties in the photodegradation of MO. A series of different secondary linkers are employed to facilitate the dimensionality of the compounds, such as benzimidazole (bm), 2-nitroterephthalic acid ($H_2$ntp) and 1,2,4-trimellitic acid ($H_3$btc). The constructed CPs are formulated as [Co(bbbi)$_{0.5}$(bm)(Hbtc)] (**32**) and [$Ag_2$(bbbi)$_2$(ntp)($H_2O$)·4$H_2O$]n (**33**); crystallographic determination for each structure reveals a ladder chain-like framework (Figure 29) for **32**, while **33** forms a zig-zag chain. Under similar conditions compared to the other photodegradation examples mentioned so far in this review (with sodium persulfate as the oxidant), both compounds catalyze the degradation of MO with moderate to very good (84% for **32**, 46% for **33**) efficiency after approximately 2 hours.

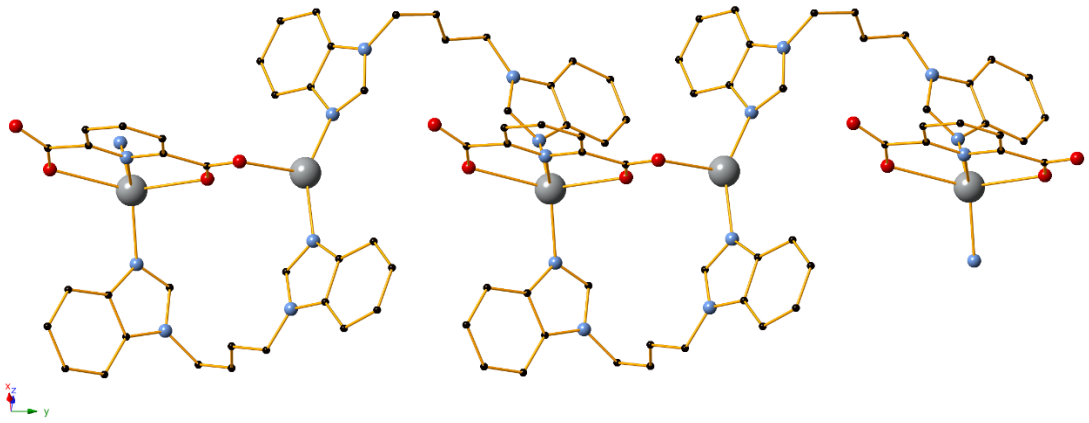

**Figure 28.** The 1D helical chain in **30**. H-atoms have been removed for clarity. Colour code Ag (grey), C (black), N (light blue), O (red).

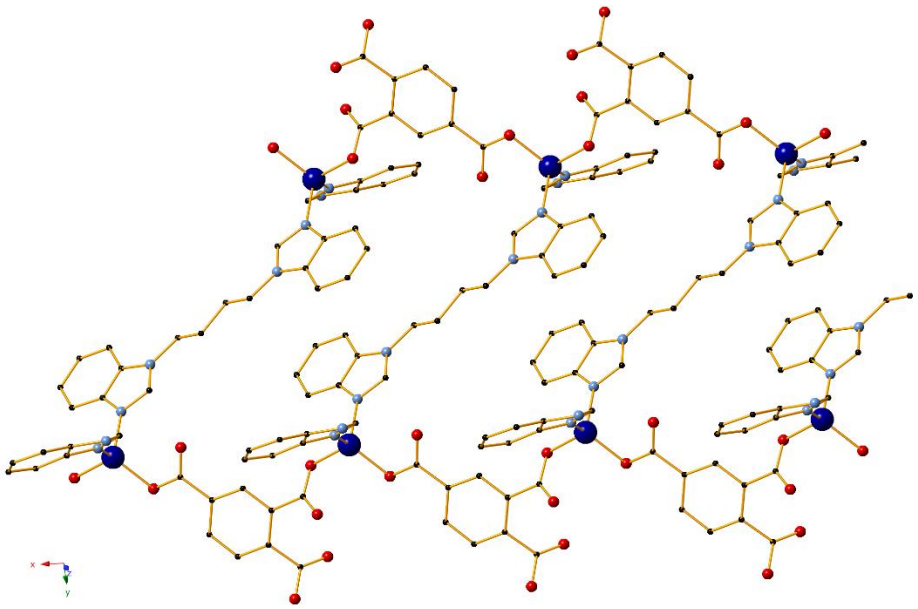

**Figure 29.** Part of the 1D ladder-like framework in **32**. Disordered atoms and H-atoms have been removed for clarity. Colour code Co (dark blue), C (black), N (light blue), O (red).

The efficiency of the photocatalysts can also be tuned through other parameters related to crystal engineering. For example, in a 2016 study by Hussain and Bhardwaj[115] the authors investigate the effect of different coordination environments by employing the formerly mentioned 1D Cu(II) coordination polymers **14**-**16** for the photodegradation of organic dyes Rhodamine B (RhB) and Methyl Orange. Investigation of their photocatalytic performance showed that all compounds catalyze efficiently the degradation of RhB and MO, with **16** exhibiting the highest performance (99% degradation of RhB, 64% degradation of MO after 2 hours). Interestingly, it is proposed that the high activity of **16** is mainly attributed to the water-rich coordination environment of the Cu(II) centers, as water coordinated complexes provide an easier access to ·OH radicals, which increases the efficiency of the photodegradation process.

In addition, a study by Wu and co-workers[116] reports a Ag(I) 1D CP as an efficient catalyst for the photodegradation of nitroaromatics. A polyphosphine-based ligand, 1,4-*N*,*N*,*N*′,*N*′-tetra(diphenylphosphanylmethyl) benzene diamine (dpppda) is used for this purpose. The compound is built from $[Ag_4(NO_3)_4]$ nodes which are linked to each other by dpppda molecules to form a 1D chain-like architecture (Figure 30). The resulting tetrasilver CP, $[Ag_4(NO_3)_4$(dpppda)] (**34**), shows very good photocatalytic performance in the degradation of the carcinogenic and toxic compounds nitrobenzene (NB), paranitrophenol (PNP) and 2,4-nitrophenol (2,4-DNP). Complete

degradation of the nitroaromatic compounds occurs under UV light exposure after 5 (for NB and PNP) or 6 hours (for 2,4-DNP) as monitored by their characteristic absorption bands. The presence of the photocatalyst is critical, as the degradation does not take place when **34** is absent. The catalyst is also easily recoverable and may be reused for at least five cycles of photodegradations. Regarding the mechanism of the reaction, the authors suggest a radical-assisted pathway as determined by several control experiments.

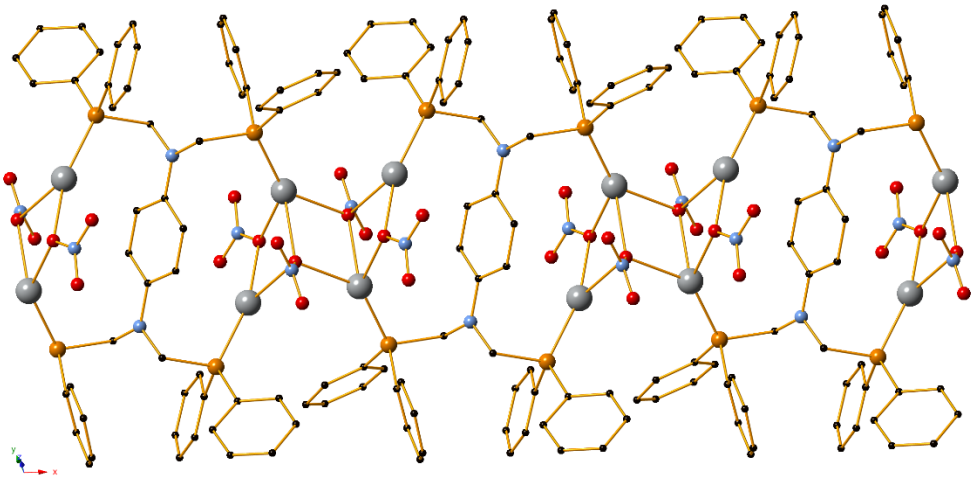

**Figure 30.** The 1D framework in **34**. H-atoms have been removed for clarity. Colour code Ag (grey), C (black), N (light blue), O (red), P (light orange).

The development of efficient methods towards the production of molecular hydrogen remains one of the biggest challenges in chemical research. Photocatalytic $H_2O$ splitting has emerged as a very promising method for this purpose, as it only requires the presence of solar energy and a catalyst to dissociate $H_2O$ into $H_2$ and $O_2$. In a series of recent studies, Downes and Marinescu reported the development of an efficient strategy towards one-dimensional CPs with remarkable $H_2$-evolution activity. The first of these works[117] involved the use of Co(II) acetate and the sulfur-based ligand benzene-1,2,4,5-tetrathiol (btt) to generate the corresponding 1D CP (**35**, Scheme 16) as confirmed by various (elemental composition analysis, XPS, FTIR, UV-Vis) studies. The compound is then immobilized onto glassy carbon electrodes resulting in a very stable metal-organic surface which exhibits excellent $H_2$-evolution activity as a heterogeneous catalyst. The concept was further investigated in following studies which included tuning of the metal source and the ligand:  The respective Ni(II), Fe(II) and Zn(II) CPs with btt were synthesized and

characterized in similar fashion[118]. While the iron and zinc analogues showed very little activity, the nickel analogue **36** provided efficient stability and hydrogen evolving performance. Furthermore, a similar selenium-based ligand, benzene-1,2,4,5-tetraselenolate (btSe) was employed to generate 1D CPs with enhanced catalytic activity[119]. Indeed, two additional compounds based on Co(II) (**37**) and Ni(II) (**38**) were synthesized; both CPs show noteworthy improvement in their catalytic performance compared to the sulfur analogues, reaching similar $H_2$-evolution activity in a much lower overpotential.

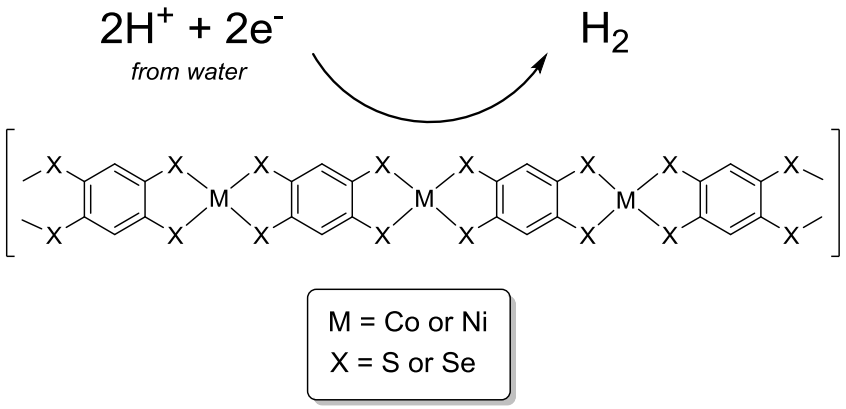


**Scheme 16.** A schematic representation of the 1D CPs with activity towards $H_2$ evolution.

Very recently, a study by Mishra and co-workers[120] surfaced, reporting a new 1D Cu(II) CP which contains the oxidized ligand 1,2-bis(diphenylphosphino)ethane dioxide (dped). The formulated compound, $[Cu_2(OAc)_4(dped)]$ (**39**), contains Cu(II) paddle wheel units derived from the starting material Cu(II) acetate; each of these metal centers is also coordinated to a dped molecule, possessing a square pyramidal geometry. This results to the formation of a 1D zig-zag framework as featured in Figure 31. It was found that **39** acts as an efficient water oxidation electrocatalyst; it also retains its stability after 12 hours of electrolysis. Interestingly, the authors propose that the coordination environment of the metal centers could affect in the catalytic activity of **39**.

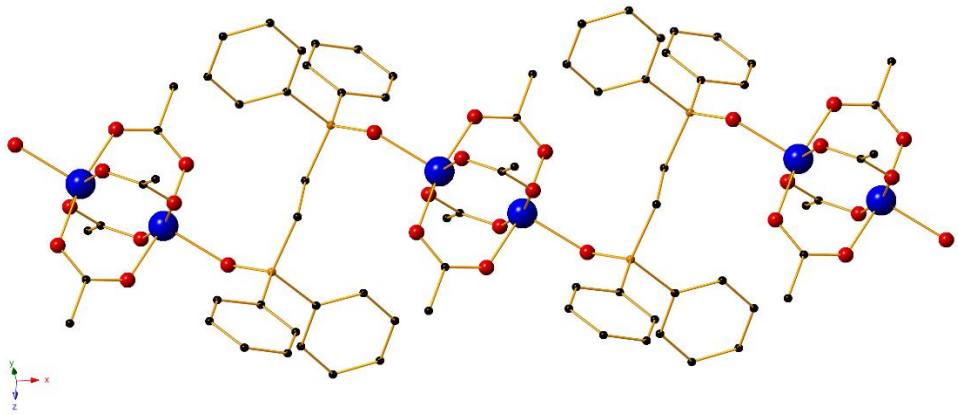

**Figure 31.** The 1D zig-zag framework in **39**. H-atoms have been removed for clarity. Colour code Cu (blue), C (black), N (light blue), O (red).

## 3. HETEROMETALLIC CPs

As the search for new and effective metal catalysts carries on, the concept of multimetallic systems has been growing increasingly[121]. The use of two or more different metal elements in order to promote a reaction can be very rewarding and enhance the catalytic performance in various ways: firstly, the potential cooperativity and synergy effects[122,123] can lead to improvements in the catalytic activity, as the multimetallic system may provide greater performance than the individual homometallic components. Furthermore, reports have shown that the binding affinity of a substrate to metal center may increase when another metal center is in close proximity[124].

In the scope of coordination chemistry, the employment of different metal elements is a common synthetic strategy for the construction of polymeric coordination compounds. In this case the building units comprise of coordination complexes (metalloligands[125]); these units are linked to each other through hetero-metallic nodes, which provide additional dimensionality to the structure. The metalloligand approach is of significant interest in catalysis, as it can efficiently provide unsaturated catalytically active metal sites. This may be further utilized or exploited by tuning the selection of ligand or the resulting coordination environment. It is therefore understandable that, amongst the many reports of multimetallic compounds with catalytic properties that have surfaced in recent years, an increasing number concerns one-dimensional coordination polymers.

The first relevant example was reported by Kirillov and co-workers[126] in 2010. The authors explored the coordination chemistry of N,N-bis(2-hydroxyethyl)-2-aminoethanesulfonic acid ($H_3$bes), a common buffer in biology. An additional co-linker, 4-hydroxybenzoic acid ($H_2$phba) as well as Cu(II) and Na(I) sources were added to generate $[Cu_4(Hbes)_4(phba)Na(H_2O)_4)]$ (**40**), a 1D zig-zag coordination polymer. **40** comprises of tetracopper $[Cu_4(Hbes)_4(phba)]$ units linked by Na-contaning nodes which provide dimensionality. This heterometallic compound showed similar coordination environment and water solubility to the enzyme methane monooxygenase, and was therefore tested in oxidation reactions. Remarkably, **40** catalyzes (Scheme 2) the oxidation of propane and n-butane to 2-butyric acid and 2-methylbutyric acid in good yields (64 and 67%). These reactions were performed in $H_2O$/MeCN and at low temperatures (50-60 $^oC$). While the role of Na is not further investigated in the study, the activity of **40** is much superior compared to other tetracopper complexes with similar coordination environment.

Bhunia and others[127] employed a targeted synthesis of Mn(II)/Ln(III) CPs based on the salen ligand N,N'-bis(4-carboxysalicylidene)ethylenediamine ($H_4$bced) to generate 1D frameworks with metal centers as active sites. The CPs were then successfully used as catalysts in the epoxidation of olefins. A total of five isostructural compounds were synthesized, formulated as $\{Ln_2[Mn(bced)Cl]_2(NO_3)_2(DMF)_5\}\cdot 4DMF$ (**41**-**45**), where Ln=Nd (**41**), Eu (**42**), Gd (**43**), Dy (**44**), Tb (**45**). The frameworks are constructed by two different Mn-based units, [Mn(bced)Cl(DMF)] and [Mn(bced)Cl], which are then connected by lanthanide-based nodes. Regarding their catalytic activity, **41**-**45** afforded similarly good (60-66%) yields and TONs (83-86) in the epoxidation of trans-stilbene with molecular oxygen in order to form stilbene oxide. Subsequent uses of the recycled catalyst showed a slight loss in yield (49% after two runs). Optimal conditions for the reaction incorporate low catalyst loadings (0.76 mol%), albeit high temperatures (150 $^oC$), and a non-environmentally friendly solvent (DMF) are also employed. Further tests were made using a zero-dimensional Mn(II) complex with a very similar salen ligand, affording significantly lower conversions. These results show that the choice of lanthanide has zero effect on the catalytic activity directly; however, its role as a secondary building unit in the generation of the 1D framework is essential in order to optimize the catalytic performance. The authors suggest that the stable framework architecture protects the ligand from oxidation, which would lead to deactivation of the catalyst. The same concept was expanded by Yadav and co-workers[128]

in an attempt to introduce chirality through slight modifications in the ligand and explore other organic transformations. The authors introduced a series of enantioselective catalysts for sulfoxidation, based on the chiral salen ligand N,N′-bis(4-carboxysalicylidene)cyclohexanediamine ($H_4$bccy) and Mn(II)/Ln(III) sources. More specifically, all compounds are isostructural, formulated as $\{Ln_2[Mn(bccy)Cl]_2(NO_3)_2(DMF)_6(H_2O)_2\}\cdot xH_2O$, where Ln = Pr (**46**), Nd (**47**), Sm (**48**) and Gd (**49**). **46**-**49** exhibit a 1D polymeric chain in which dilanthanide nodes connect the chiral manganese-based metalloligands and extend the framework along the axis (Figure 32). These chiral CPs were then found to catalyze the sulfoxidation of both aryl and alkyl sulfides (Scheme 7), when iodosobenzene is used as the oxidizing agent. Only 1 mol% of the CP catalyst is required, while no inert atmosphere is needed. Similarly with the olefin epoxidation Mn/Ln catalysts, the choice of the lanthanide element does not play a role in the catalysis, as **46**-**49** provided very similar yields of the sulfoxides. While the catalysts provide moderate to excellent (36-100%) yields of the products, the corresponding results regarding enantioselectivity were less encouraging (ee up to 25%).

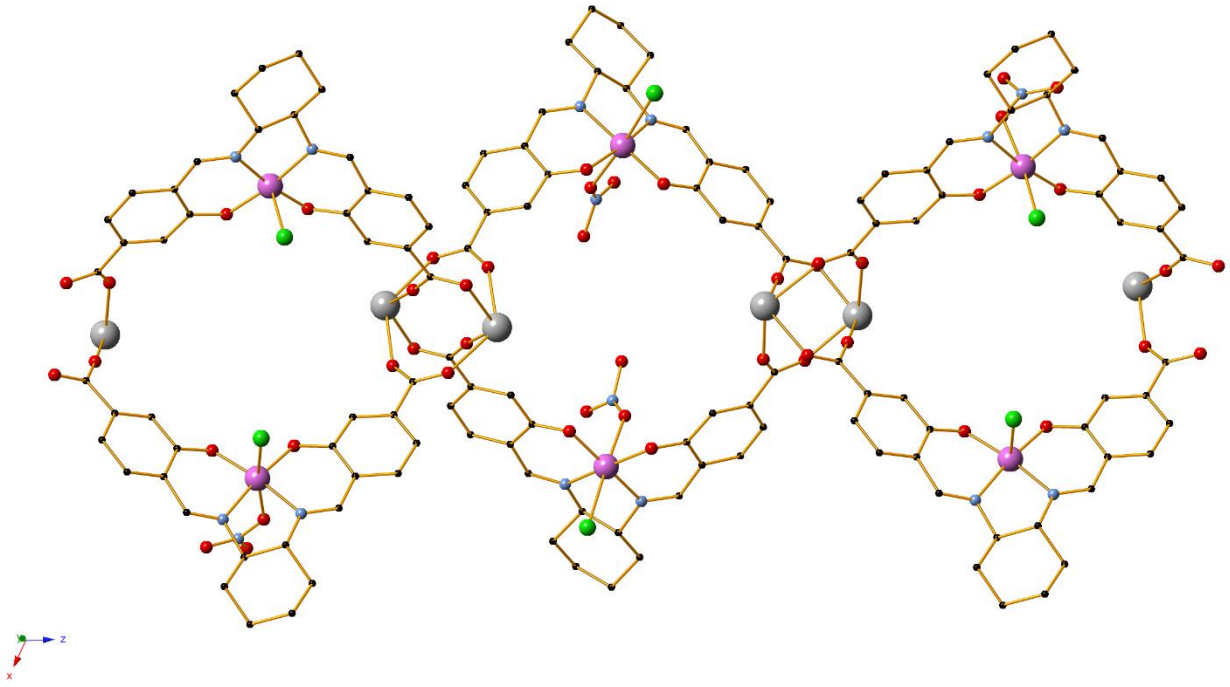

**Figure 32.** The 1D polymeric framework found in compounds **46**-**49**. DMF molecules and H-atoms have been removed for clarity. Colour code Mn (pink), Ln (grey), C (black), N (light blue), O (red).

Another heterometallic one-dimensional coordination polymer based on a lanthanide element is presented by Kumar and co-workers[129] in a recent study. The CP contains a Co(III)/Eu(III) core and was found to be a suitable catalyst for various ring opening reactions of epoxides. The metalloligand approach is once again used in the synthetic method, as a Co(III) precursor with the ligand 4,4'-((pyridine-2,6-dicarbonyl)bis(azanediyl))dibenzoic acid ($H_4$pdada) is employed. Addition of the lanthanide source follows, as the 1D CP $[Co(pdada)_2Eu(H_2O)_5]\cdot 8H_2O$ (**50**) is constructed (Figure 33). Each metalloligand as a whole coordinates to two Eu(III) centers, generating a zig-zag framework. The compound was then used successfully as a heterogeneous catalyst in the ring opening reactions of cyclohexene oxide and styrene oxide with various nucleophiles (Scheme 17), including anilines (aminolysis), trimethylsilyl azide (azidolysis), alcohols (alcoholysis) and thiols (thialysis). The corresponding products are afforded at excellent yields (78-100%) and under mild conditions, as the reactions are treated with 2 mol% catalyst under ambient conditions and for 4 hours. Reusability tests showed that the catalyst may be recycled at least five times with very minor losses in yield. The activity of this heterometallic CP is mainly attributed to the strong Lewis acidic nature of the Eu(III) centers, as well as their coordinating environment. Many of the coordination sites of the lanthanide are occupied by labile water molecules, providing an easy access to substrates.

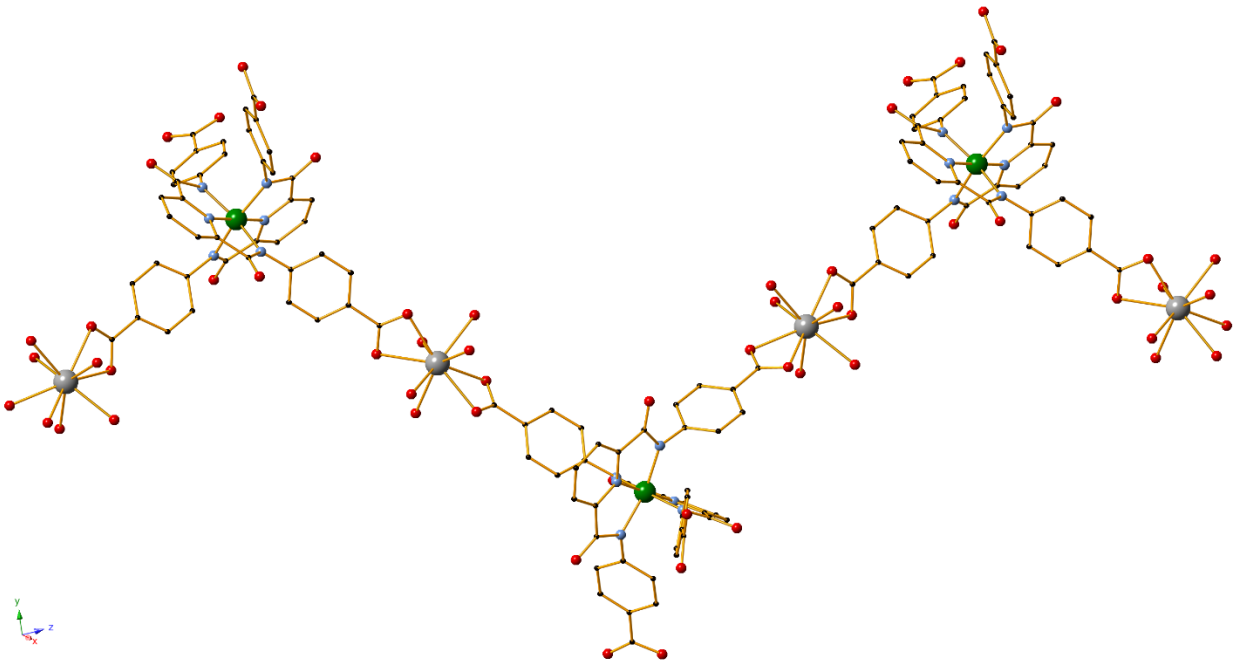

**Figure 33.** Part of the zig-zag chain in **50**. Lattice solvent molecules and H-atoms have been removed for clarity. Colour code Co (green), Eu (grey), C (black), N (light blue), O (red).

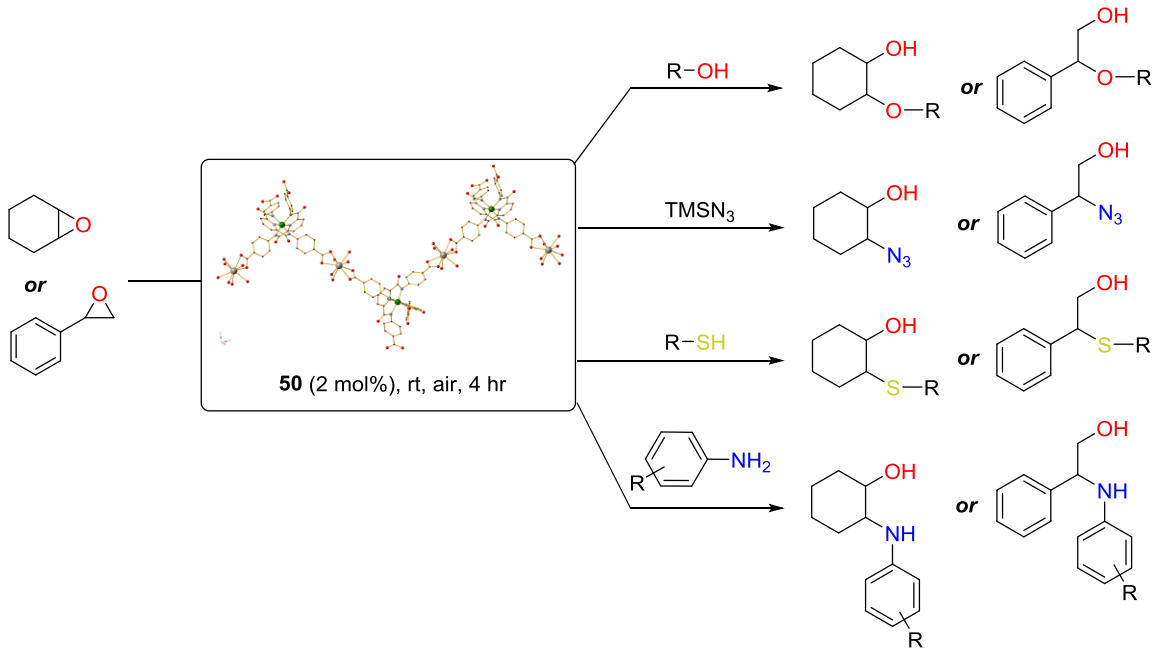


**Scheme 17.** A scope of the ring-opening reactions catalyzed by **50**.

Hou and co-workers[130] developed a Cu(I)/Cu(II) 1D coordination polymer with interesting multifunctional catalytic properties. The CP was constructed through post-synthetic modification methods using the salen ligand N,N'-bis-[(imidazol-4-yl)methylene]cyclohexane-1,2-diamine ($H_2$icyd). Initially, a zero-dimensional [$Cu^{II}$($H_2$icyd)]·2($NO_3$) metalloligand was assemblied and characterized. Addition of Cu(I) iodide under solvothermal conditions led to a targeted CP, [$Cu^{II}$(icyd)($Cu^{I}$I)]·2DMF (**51**), that propagates into one dimension through Cu(I)-halide bridging which links the metalloligand units (Figure 34). The resulting heterometallic CP contains trigonal Cu(I) and square planar Cu(II) centers, both of which are unsaturated. The catalytic activity of **51** was firstly examined in the asymmetric Strecker synthesis, a multicomponent reaction towards the synthesis of α-aminonitriles (Scheme 18). Remarkable conversions of 86 to 99% were achieved using various aromatic aldehydes, TMSCN and the asymmetric amine (R)-(+)-1-phenylethylamine; typical conditions include the presence of **51** at only 0.5 mol%, in $CD_3CN$ at 10$^o$C for 1-3 hours. This method also provided encouraging results regarding diastereoselectivity (R,R:R,S up to 71:29). Furthermore, the solid catalyst may be recovered through a simple centrifugation and be reused up to three cycles retaining a high (95%) conversion. The performance of other comparable catalysts was then evaluated in order to determine the effect of the different metal centers; reference catalysts included $I_2$, $Cu^{I}$I, the zero-dimensional

$[Cu^{II}(H_2icyd)]\cdot 2(NO_3)$ metalloligand and the dual catalytic system $[Cu^{II}(H_2icyd)]\cdot 2(NO_3)$ / $Cu^{I}I$. All compounds provided much lower activity compared to **51**, indicating that a cooperative effect takes place between the Cu(I) and Cu(II) metal centers of the coordination polymer. It is proposed that the unsaturated Cu(I) centers, which possess a $\{I_2N\}$ coordination environment, function as Brønsted bases to activate the cyanides; concurrently, the unsaturated Cu(II) sites act as Lewis acids and activate the imine intermediates formed by the aldehyde and the amine.

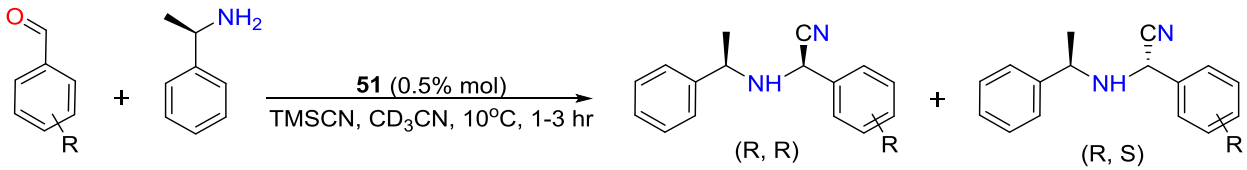


**Scheme 18.** The Strecker reaction as catalyzed by **51**.

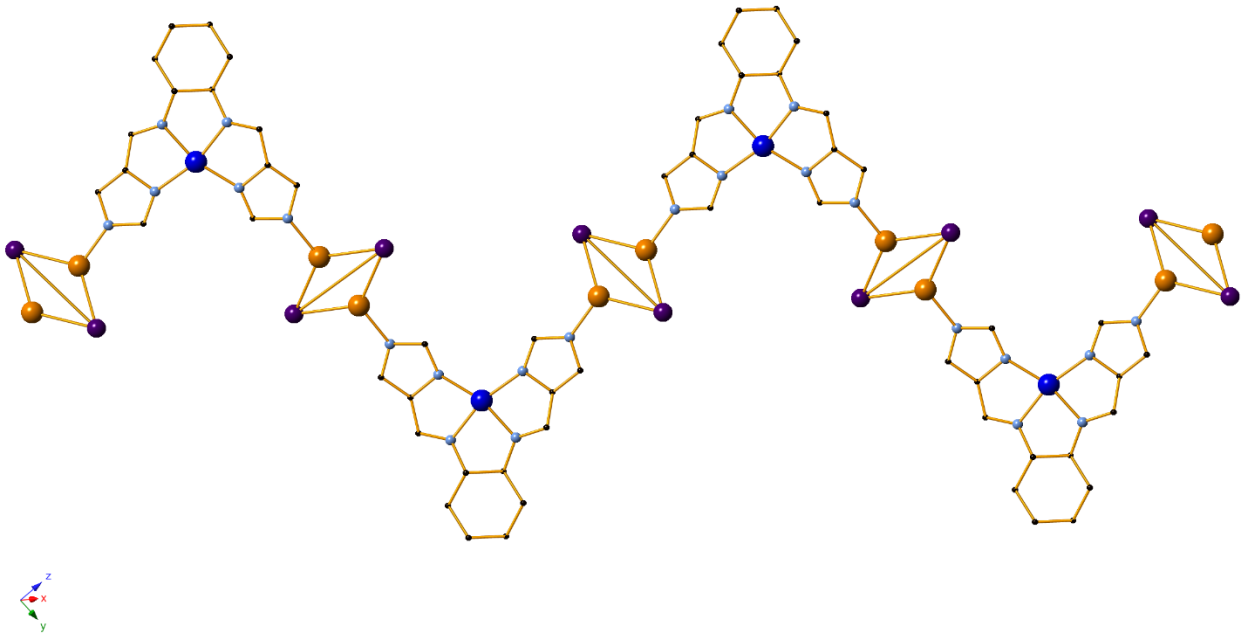

**Figure 34.** The 1D framework formed in compound **51**. Lattice solvent molecules and H-atoms have been removed for clarity. Colour code $Cu^{II}$ (blue), $Cu^{I}$ (light orange), C (black), N (light blue), I (purple).

**51** was also employed in the catalytic photodegradation of the organic dyes methylene blue (MB), RhB and MO. Investigation by UV-Vis spectroscopy showed that **51** achieves excellent (up to 96%) photocatalytic efficiency in all cases, after 50-55 minutes of light illumination.

Additionally, the solid catalyst retains similar efficiency after three cycles. For the case of MB, it is suggested that while the Cu(II) centers of **51** are essential for the oxidation of the dye compound, the reaction is further enhanced by the photoactive Cu(I) moieties leading to a cooperative degradation.

Very recently, Kuwamura and co-workers[131] reported an uncommon case of a trimetallic 1D CP based on Pt(II), Pd(II) and Ni(II), which shows catalytic activity in hydrogen evolution electrochemical reactions. For the construction of the CP the authors employ a stepwise metalloligand approach; first, the *trans*-$[Pt(NH_3)_2(D\text{-}pen)_2]$ complex is generated (D-$H_2$pen = D-penicillamine) and then treated with Pd(II) acetate to afford a 0D compound containing a tetranuclear $Pt_2Pd_2$ core. The oxygen-containing coordination sites of D-pen are then utilized by the introduction of nickel and the resulting CP $[\{Pd_2Pt_2(NH_3)_4(D\text{-}pen)_4\}\{Ni(H_2O)_4\}]\cdot Cl_2$ (**52**) is formed (Figure 35). Interestingly, evolution of $H_2$ gas from the electrode surface was observed during voltammetry experiments for **52** in a $H_2O$/MeCN solvent system. As no effect was noted in similar experiments under absolute MeCN, **52** therefore acts as a heterogeneous catalyst for the electrochemical reduction of water. When tested for their $H_2$ evolution activity under similar conditions, the $[Pd_2Pt_2(NH_3)_4(D\text{-}pen)_4]$ and $[Pt(NH_3)_2(D\text{-}pen)_2]$ complexes are much inferior to **52**, indicating that a cooperative effect between all three metal elements takes place in order to improve the performance of the catalyst.

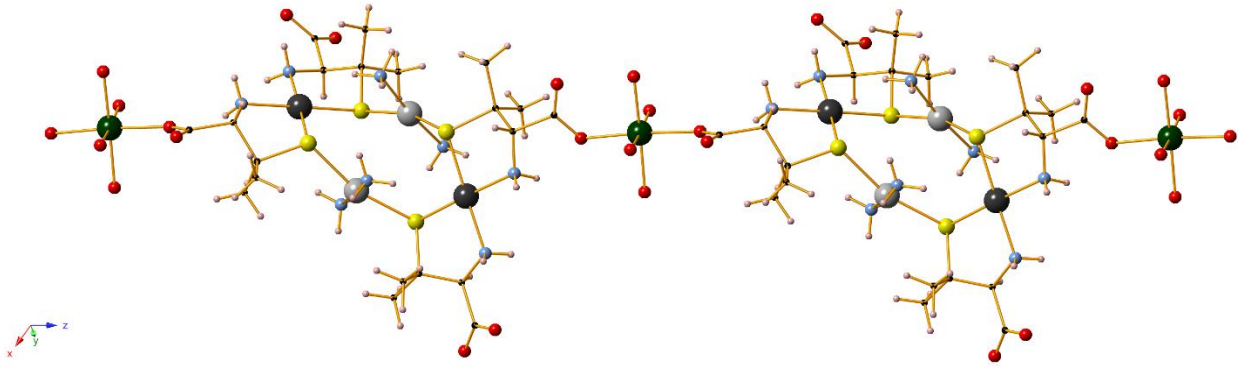

**Figure 35.** The trimetallic 1D framework in **52**. Chlorine atoms have been removed for clarity. Colour code Ni (green), Pd (dark grey), Pt (grey), C (black), N (light blue), O (red), S (yellow), H (light pink).

## 4. SUMMARY AND CONCLUDING REMARKS

In this review we have attempted to report 1D CPs with catalytic activity in organic transformations that have appeared in the literature over the last ten years. All relevant synthetic and catalytic aspects are discussed in this review in detail. It is worth noting that the majority of reported studies in this summary are from 2015 and onwards; therefore it is clear that the field will continue to expand in the following years.

The increased attention and utilization of 1D CPs is in no small part due to their unique characteristics and advantages. Synthetic-wise, they provide easier assembly compared to the more frequently used 3D porous MOFs which typically require solvothermal conditions. Indeed, most of the reported compounds in this review were generated under very mild conditions and in high yields. Furthermore, 1D CPs offer a possibly endless work area through the plethora of available options in ligand and metal selection, allowing for their incredible structural flexibility; as such, the compounds presented in this study are based on many different transition metals (Cu(I), Cu(II), Ni(II), Co(II), Mn(II) Zn(II), Ag(I), Sn(IV), La(III) etc.) and employ a large variety of ligands that ranges from Schiff bases and salen analogues to carboxylate linkers and nitrogen-based heterocyclic molecules. The diversity in options has been exploited in the reported studies in great effect, through the use of i) pre-synthetic ligand design towards CPs with intended solubility that may act as homogeneous or heterogeneous (and sometimes green) catalysts ii) post-synthetic modifications to generate targeted CPs and optimize their potential, iii) suitable ligands to mimic the coordination sphere of common catalysts and enzymes, iv) ligand and metalloligand tuning to introduce chirality, specific metal geometries or unsaturated active sites, v) multimetallic CPs to provide synergistic and cooperative effects. As a result, the use of 1D CPs in many of these studies achieves unparalleled optimization of the catalyst and its performance. Indeed, several of the reported catalysts referred in this review were found to outperform 3D MOFs with analogous reported activity during screening tests.

The polymeric nature of these materials also appears to be an important factor which affects the catalytic performance. The constructed networks are typically robust and show increased thermal stability over analogous discrete zero-dimensional compounds, as well as larger endurance under adverse conditions. These advantages are crucial in organic reactions which involve very high temperatures or extreme conditions, contributing to the high catalytic activity. In many cases it is also very important that the polymeric precursors are well defined and formed before the reaction occurs, in order to achieve optimal catalytic performance. This was demonstrated in

several studies where the analogous *in situ* formation of the catalyst led to other species that were less active. Furthermore, CPs may provide a larger number of unsaturated active sites and enhance the catalytic performance against separated monomers/dimers or simple metal salts. The increased control and refinement of structural parameters in the case of 1D CPs allows for additional catalytic superiority. As a result, coordination aspects such as metal geometry and environment appear to be crucial in multiple cases in this review. Unique topological features for 1D CPs are also reported to play a role: as a notable example, the high activity of **29** in aldehyde cyanosilylation may be associated to its 1D zig-zag structure which provides easy access to its Lewis-acid Zn(II) sites. Other reports involve the formation of weak interactions that are mechanistically crucial to the catalysis and can only be formed in a 1D polymeric architecture. Compounds **2** and **17** are characteristic examples of this behaviour. Finally, as seen in the case of compound **52**, the polymeric nature may also be important for multimetallic complexes, as it increases the required synergistic effects; the metalloligand approach is therefore ideal for these type of catalysts.

On the other hand, despite the evident potential of low-dimensional materials in catalysis, significant issues remain unresolved. Important steps have been made in the last decades towards improved crystal engineering and rational design of CPs, however controlling and predicting the final products of the self-assembly procedure still remains one of the major challenges in the field. In this situation, the increased flexibility and variety of 1D CPs is more of a disadvantage compared to rigid 3D MOFs. Important points can also be raised about the limitations of 1D CPs, as their exact role in the catalysis is, in some cases, vague: in several reports of this review the mechanistic details are still unclear, or in the case of some homogeneous catalysts the nature of the active catalytic species remains undetermined. In addition, while the catalytic activity of the compounds is generally compared to the performance of analogous 3D MOFs, few of these studies perform similar comparisons with the relevant zero-dimensional compounds. For these reasons, we believe future developments should focus on more systematic efforts towards a conclusive rational design of multifunctional catalysts; these catalysts should be well defined and characterized due to the large number of parameters involved. We believe that the field still has plenty of room for improvement and offers exciting possibilities for catalyst development. While the regular use of 1D CPs as catalysts still seems far away, the subject is definitely on the rise and its future can only be bright.

## 5. REFERENCES


1 S. R. Batten, N. R. Champness, X.-M. Chen, J. Garcia-Martinez, S. Kitagawa, L. Öhrström, M. O'Keeffe, M. P. Suh and J. Reedijk, *CrystEngComm*, 2012, **14**, 3001.

2 S. R. Batten, N. R. Champness, X.-M. Chen, J. Garcia-Martinez, S. Kitagawa, L. Öhrström, M. O'Keeffe, M. Paik Suh and J. Reedijk, *Pure Appl. Chem.*, 2013, **85**, 1715–1724.

3 J. C. Bailar Jr., in *Preparative Inorganic Reactions. Volume 1.*, Interscience Publishers, John Wiley and Sons, New York, 1964, vol. 1, pp. 1–25.

4 B. F. Hoskins and R. Robson, *J. Am. Chem. Soc.*, 1989, **111**, 5962–5964.

5 B. F. Hoskins and R. Robson, *J. Am. Chem. Soc.*, 1990, **112**, 1546–1554.

6 S. R. Batten, B. F. Hoskins and R. Robson, *J. Chem. Soc. Chem. Commun.*, 1991, **0**, 445.

7 B. F. Abrahams, B. F. Hoskins, J. Liu and R. Robson, *J. Am. Chem. Soc.*, 1991, **113**, 3045–3051.

8 S. Kitagawa, S. Matsuyama, M. Munakata and T. Emori, *J. Chem. Soc. Dalt. Trans.*, 1991, **0**, 2869–2874.

9 B. F. Abrahams, M. J. Hardie, B. F. Hoskins, R. Robson and G. A. Williams, *J. Am. Chem. Soc.*, 1992, 114, 10641–10643.

10 G. R. Desiraju, *J. Am. Chem. Soc.*, 2013, **135**, 9952–67.

11 G. R. Desiraju, *Angew. Chemie Int. Ed. English*, 1995, **34**, 2311–2327.

12 K. R. Seddon and M. Zaworotko, *Crystal Engineering: The Design and Application of Functional Solids, Volume 539*, Springer Science & Business Media, 1999.

13 B. Moulton and M. J. Zaworotko, *Chem. Rev.*, 2001, 101, 1629–1658.

14 C. N. Morrison, A. K. Powell and G. E. Kostakis, *Cryst. Growth Des.*, 2011, **11**, 3653–3662.

15 J. Chen, N. Voutier, J. Rajabi, A. Crochet, D. M. Bassani and K. M. Fromm, *CrystEngComm*, 2017, **19**, 5106–5113.

16 S. I. Noro, J. Mizutani, Y. Hijikata, R. Matsuda, H. Sato, S. Kitagawa, K. Sugimoto, Y. Inubushi, K. Kubo and T. Nakamura, *Nat. Commun.*, 2015, **6**, 5851.

17 I. Burneo, K. Stylianou, I. Imaz and D. Maspoch, *Chem. Commun.*, 2014, **50**, 13829–13832.

18 L. A. Dubraja, K. Imir, M. Anov, D. Žili, B. Koji-Prodi and E. Wenger, *New J. Chem.*

*New J. Chem*, 2017, **41**, 6785–6794.

19 X. Liu, P. Cen, H. Li, H. Ke, S. Zhang, Q. Wei, G. Xie, S. Chen and S. Gao, *Inorg. Chem.*, 2014, **53**, 8088–8097.

20 S. K. Ghosh and S. Kitagawa, *CrystEngComm*, 2008, **10**, 1739.

21 Y.-F. Hou, B. Liu, K.-F. Yue, C.-S. Zhou, Y.-M. Wang, N. Yan and Y.-Y. Wang, *CrystEngComm*, 2014, **16**, 9560–9567.

22 C. Huang, X. Han, Z. C. Shao, K. Gao, M. Liu, Y. Wang, J. Wu, H. Hou and L. Mi, *Inorg. Chem.*, 2017, **56**, 4874–4884.

23 L.-Y. Du, W.-J. Shi, L. Hou, Y.-Y. Wang, Q.-Z. Shi and Z. Zhu, *Inorg. Chem.*, 2013, **52**, 14018–27.

24 Y. Y. Yin, J. G. Ma, Z. Niu, X. C. Cao, W. Shi and P. Cheng, *Inorg. Chem.*, 2012, **51**, 4784–4790.

25 L. Bello, M. Quintero, A. J. Mora, T. González, A. Escalona, R. Añez, E. E. Ávila and A. Briceño, *CrystEngComm*, 2015, **17**, 5921–5931.

26 A. Aijaz, P. Lama and P. K. Bharadwaj, *Inorg. Chem.*, 2010, **49**, 5883–5889.

27 L. Hashemi, A. Morsali and S. W. Joo, *Dalt. Trans.*, 2014, **43**, 1489–1492.

28 B. Manna, A. V. Desai, N. Kumar, A. Karmakar and S. K. Ghosh, *CrystEngComm*, 2015, **4**, 1166–1169.

29 N. Koiso, Y. Kitagawa, T. Nakanishi, K. Fushimi and Y. Hasegawa, *Inorg. Chem.*, 2017, **56**, 5741–5747.

30 J. Y. Wu, C. Y. Chang, C. J. Tsai and J. J. Lee, *Inorg. Chem.*, 2015, **54**, 10918–10924.

31 J. Shi, Y. Zhang, B. Zhang and D. Zhu, *Dalt. Trans.*, 2016, **45**, 89–92.

32 M. H. Weston, W. Morris, P. W. Siu, W. J. Hoover, D. Cho, R. K. Richardson and O. K. Farha, *Inorg. Chem.*, 2015, **54**, 8162–8164.

33 J. Yu, L.-H. Xie, J.-R. Li, Y. Ma, J. M. Seminario and P. B. Balbuena, *Chem. Rev.*, 2017, **117**, 9674–9754.

34 S. Rojas, F. J. Carmona, C. R. Maldonado, P. Horcajada, T. Hidalgo, C. Serre, J. A. R. Navarro and E. Barea, *Inorg. Chem.*, 2016, **55**, DOI: 10.1021/acs.inorgchem.6b00045.

35 P. Horcajada, C. Serre, M. Vallet-Regí, M. Sebban, F. Taulelle and G. Férey, *Angew. Chem. Int. Ed. Engl.*, 2006, **45**, 5974–8.

36 T.-T. Zheng, J. Zhao, Z.-W. Fang, M.-T. Li, C.-Y. Sun, X. Li, X.-L. Wang and Z.-M. Su,

*Dalt. Trans.*, 2017, **46**, 2456–2461.

37 J.-C. G. Bünzli, *Coord. Chem. Rev.*, 2015, **293**–**294**, 19–47.

38 M. H. Zeng, Z. Yin, Y. X. Tan, W. X. Zhang, Y. P. He and M. Kurmoo, *J. Am. Chem. Soc.*, 2014, **136**, 4680–4688.

39 S. L. Anderson and K. C. Stylianou, *Coord. Chem. Rev.*, 2017, 349, 102–128.

40 D. Liu, K. Lu, C. Poon and W. Lin, *Inorg. Chem.*, 2014, **53**, 1916–24.

41 B. Li, H. M. Wen, Y. Cui, W. Zhou, G. Qian and B. Chen, *Adv. Mater.*, 2016, 28, 8819–8860.

42 O. M. Yaghi, G. Li and H. Li, *Nature*, 1995, **378**, 703–706.

43 O. M. Yaghi and H. Li, *J. Am. Chem. Soc.*, 1995, **117**, 10401–10402.

44 E. Loukopoulos, K. Griffiths, G. Akien, N. Kourkoumelis, A. Abdul-Sada and G. Kostakis, *Inorganics*, 2015, **3**, 448–466.

45 S. W. Jaros, J. Sokolnicki, A. Wołoszyn, M. Haukka, A. M. Kirillov and P. Smoleński, *J. Mater. Chem. C*, 2017.

46 T. A. Fernandes, C. I. M. Santos, V. André, J. Kłak, M. V. Kirillova and A. M. Kirillov, *Inorg. Chem.*, 2016, **55**, 125–135.

47 X. Huang, P. Sheng, Z. Tu, F. Zhang, J. Wang, H. Geng, Y. Zou, C. A. Di, Y. Yi, Y. Sun, W. Xu and D. Zhu, *Nat. Commun.*, 2015, **6**, 7408.

48 E. Loukopoulos, N. F. Chilton, A. Abdul-Sada and G. E. Kostakis, *Cryst. Growth Des.*, 2017, **17**, 2718–2729.

49 K. Banerjee and K. Biradha, *New J. Chem.*, 2016, **40**, 1997–2006.

50 R. A. Agarwal, *Sci. Rep.*, 2017, **7**, 13212.

51 J.-X. Yang, Y.-Y. Qin, J.-K. Cheng, X. Zhang and Y.-G. Yao, *Cryst. Growth Des.*, 2015, **15**, 2223–2234.

52 T. K. Maji, R. Matsuda and S. Kitagawa, *Nat. Mater.*, 2007, **6**, 142–8.

53 C. T. Chen and K. S. Suslick, *Coord. Chem. Rev.*, 1993, **128**, 293–322.

54 W. L. Leong and J. J. Vittal, *Chem. Rev.*, 2011, **111**, 688–764.

55 C. Slabbert and M. Rademeyer, *Coord. Chem. Rev.*, 2015, 288, 18–49.

56 Y. Y. Karabach, A. M. Kirillov, M. Haukka, M. N. Kopylovich and A. J. L. Pombeiro, *J. Inorg. Biochem.*, 2008, **102**, 1190–1194.

57 R. Jlassi, A. P. C. Ribeiro, M. F. C. Guedes Da Silva, K. T. Mahmudov, M. N.

Kopylovich, T. B. Anisimova, H. Na??li, G. A. O. Tiago and A. J. L. Pombeiro, *Eur. J. Inorg. Chem.*, 2014, **2014**, 4541–4550.

58 A. Paul, A. P. C. Ribeiro, A. Karmakar, M. F. C. Guedes da Silva and A. J. L. Pombeiro, *Dalt. Trans.*, 2016, **45**, 12779–12789.

59 X. Wang, M. Liu, Y. Wang, H. Fan, J. Wu, C. Huang and H. Hou, *Inorg. Chem.*, 2017, acs.inorgchem.7b02106.

60 W. Zhang, J. L. Loebach, S. R. Wilson and E. N. Jacobsen, *J. Am. Chem. Soc.*, 1990, **112**, 2801–2803.

61 E. N. Jacobsen, W. Zhang, A. R. Muci, J. R. Ecker and L. Deng, *J. Am. Chem. Soc.*, 1991, **113**, 7063–7064.

62 K. J. O'Connor, S. J. Wey and C. J. Burrows, *Tetrahedron Lett.*, 1992, **33**, 1001–1004.

63 A. Murphy, G. Dubois and T. D. P. Stack, *J. Am. Chem. Soc.*, 2003, **125**, 5250–5251.

64 I. Garcia-Bosch, X. Ribas and M. Costas, *Adv. Synth. Catal.*, 2009, **351**, 348–352.

65 O. Cussó, I. Garcia-Bosch, X. Ribas, J. Lloret-Fillol and M. Costas, *J. Am. Chem. Soc.*, 2013, **135**, 14871–14878.

66 C. Wang and H. Yamamoto, *J. Am. Chem. Soc.*, 2014, **136**, 1222–1225.

67 R. A. Moretti, J. Du Bois and T. D. P. Stack, *Org. Lett.*, 2016, **18**, 2528–2531.

68 Y. Huang, T. Liu, J. Lin, J. Lu, Z. Lin and R. Cao, *Inorg. Chem.*, 2011, **50**, 2191–2198.

69 S. Lymperopoulou, M. Papastergiou, M. Louloudi, C. P. Raptopoulou, V. Psycharis, C. J. Milios and J. C. Plakatouras, *Eur. J. Inorg. Chem.*, 2014, **2014**, 3638–3644.

70 L. M. D. R. S. Martins, S. Hazra, M. F. C. da Silva and A. J. L. Pombeiro, *RSC Adv.*, 2016, **6**, 78225–78233.

71 S. Hazra, L. M. D. R. S. Martins, M. F. C. Guedes da Silva and A. J. L. Pombeiro, *Inorganica Chim. Acta*, 2017, **455**, 549–556.

72 Z.-H. Zhang, X.-S. Yang, Q.-Q. Zhang, L. Wang, M.-Y. He, Q. Chen and X.-F. Huang, *RSC Adv.*, 2016, **6**, 104036–104040.

73 L. Mandal, S. Mandal and S. Mohanta, *New J. Chem.*, 2017, **41**, 4689–4701.

74 M. A. Wani, A. Kumar, M. D. Pandey and R. Pandey, *Polyhedron*, 2017, **126**, 142–149.

75 N. Hussain, P. Joshi, S. R. Ali and V. K. Bhardwaj, *RSC Adv.*, 2016, **6**, 61528–61535.

76 N.-X. Zhu, C.-W. Zhao, J. Yang, X.-R. Wang, J.-P. Ma and Y.-B. Dong, *RSC Adv.*, 2016, **6**, 108645–108653.

77 S. M. F. Vilela, A. D. G. Firmino, R. F. Mendes, J. A. Fernandes, D. Ananias, A. A. Valente, H. Ott, L. D. Carlos, J. Rocha, J. P. C. Tomé and F. A. Almeida Paz, *Chem. Commun.*, 2013, **49**, 6400.

78 R. F. Mendes, P. Silva, M. M. Antunes, A. A. Valente and F. A. Almeida Paz, *Chem. Commun.*, 2015, **51**, 10807–10810.

79 M. Kallitsakis, E. Loukopoulos, A. Abdul-Sada, G. J. Tizzard, S. J. Coles, G. E. Kostakis and I. N. Lykakis, *Adv. Synth. Catal.*, 2017, **359**, 138–145.

80 C. B. Toal, P. A. Meredith and H. L. Elliott, *Blood Press.*, 2012, **21 Suppl 1**, 3–10.

81 D. R. Abernethy, J. Gutkowska and L. M. Winterbottom, *Clin. Pharmacol. Ther.*, 1990, **48**, 76–86.

82 M. B. Murphy, A. J. Scriven and C. T. Dollery, *Br. Med. J. (Clin. Res. Ed).*, 1983, **287**, 257–259.

83 K. Tanaka, T. Niino, T. Ishihara, A. Takafuji, T. Takayama, Y. Kanda, T. Sugizaki, F. Tamura, S. Kurotsu, M. Kawahara and T. Mizushima, *Sci. Rep.*, 2017, **7**, 3439.

84 A. Czyrak, E. Mogilnicka and J. Maj, *Neuropharmacology*, 1989, **28**, 229–33.

85 Y. Watanabe, H. Takano, A. Kiue, K. Kohno and M. Kuwano, *Anticancer. Drug Des.*, 1991, **6**, 47–57.

86 H.-A. S. Abbas, W. A. El Sayed and N. M. Fathy, *Eur. J. Med. Chem.*, 2010, **45**, 973–82.

87 B. Jansone, I. Kadish, T. van Groen, U. Beitnere, D. R. Moore, A. Plotniece, K. Pajuste and V. Klusa, *PLoS One*, 2015, **10**, e0127686.

88 S. Bahekar and D. Shinde, *Acta Pharm.*, 2002, **52**, 281–287.

89 H. Komoda, T. Inoue and K. Node, *Clin. Exp. Hypertens.*, 2010, **32**, 121–8.

90 A. R. Hantzsch, *Justus Liebigs Ann. Chem.*, 1882, **215**, 1–82.

91 J.-P. Wan and Y. Liu, *RSC Adv.*, 2012, **2**, 9763.

92 Y. Deng, L. Liu, R. G. Sarkisian, K. Wheeler, H. Wang and Z. Xu, *Angew. Chemie - Int. Ed.*, 2013, **52**, 3663–3667.

93 W. Gati, M. M. Rammah, M. B. Rammah, F. Couty and G. Evano, *J. Am. Chem. Soc.*, 2012, **134**, 9078–9081.

94 E. Loukopoulos, M. Kallitsakis, N. Tsoureas, A. Abdul-Sada, N. F. Chilton, I. N. Lykakis and G. E. Kostakis, *Inorg. Chem.*, 2017, **56**, 4898–4910.

95 B. M. Nilsson and U. Hacksell, *J. Heterocycl. Chem.*, 1989, **26**, 269–275.

96 D. P. Chauhan, S. J. Varma, A. Vijeta, P. Banerjee and P. Talukdar, *Chem Commun*, 2014, **50**, 323–325.

97 Y. Zhao, X. Zhou, T. Okamura, M. Chen, Y. Lu, W.-Y. Sun and J.-Q. Yu, *Dalt. Trans.*, 2012, **41**, 5889.

98 D. A. Evans, D. Seidel, M. Rueping, H. W. Lam, J. T. Shaw and C. W. Downey, *J. Am. Chem. Soc.*, 2003, **125**, 12692–12693.

99 S. Hazra, A. Karmakar, M. de F. C. Guedes da Silva, L. Dlháň, R. Boča and A. J. L. Pombeiro, *New J. Chem.*, 2015, **39**, 3424–3434.

100 A. Karmakar, M. F. C. Guedes Da Silva, S. Hazra and A. J. L. Pombeiro, *New J. Chem.*, 2015, **39**, 3004–3014.

101 N. M. R. Martins, K. T. Mahmudov, M. F. C. G. da Silva, L. M. D. R. S. Martins, F. I. Guseinov and A. J. L. Pombeiro, *Catal. Commun.*, 2016, **87**, 49–52.

102 E. Knoevenagel, *Berichte der Dtsch. Chem. Gesellschaft*, 1898, **31**, 2596–2619.

103 A. Karmakar, G. M. D. M. Rúbio, M. F. C. Guedes da Silva, S. Hazra and A. J. L. Pombeiro, *Cryst. Growth Des.*, 2015, **15**, 4185–4197.

104 E. Larrea, R. Fernández de Luis and M. Arriortua, *Molecules*, 2016, **21**, 1651.

105 Y. Li, B. He, B. Qin, X. Feng and G. Zhang, *J. Org. Chem.*, 2004, **69**, 7910–7913.

106 D. H. Ryu and E. J. Corey, *J. Am. Chem. Soc.*, 2004, **126**, 8106–8107.

107 A. Karmakar, A. Paul, G. M. D. M. Rúbio, M. F. C. Guedes da Silva and A. J. L. Pombeiro, *Eur. J. Inorg. Chem.*, 2016, **2016**, 5557–5567.

108 Z. Ma, A. V. Gurbanov, M. Sutradhar, M. N. Kopylovich, K. T. Mahmudov, A. M. Maharramov, F. I. Guseinov, F. I. Zubkov and A. J. L. Pombeiro, *Mol. Catal.*, 2017, **428**, 17–23.

109 A. Fuerte, M. D. Hernández-Alonso, A. J. Maira, A. Martinez-Arias, M. Fernandez-Garcia, J. C. Conesa and J. Soria, *Chem. Commun.*, 2001, **0**, 2718–2719.

110 X. Y. Wang, Z. Fang and X. Lin, *J. Nanoparticle Res.*, 2009, **11**, 731–736.

111 T. Wen, D.-X. Zhang, J. Liu, R. Lin and J. Zhang, *Chem. Commun.*, 2013, **49**, 5660.

112 J.-C. Geng, L. Qin, X. Du, S.-L. Xiao and G.-H. Cui, *Zeitschrift für Anorg. und Allg. Chemie*, 2012, **638**, 1233–1238.

113 W. L. Hou, G.-Y. Dong, Y. Q. Zhao and W.-G. Zhang, *Synth. React. Inorganic, Met. Nano-Metal Chem.*, 2013, **43**, 1186–1189.

114 L. Qin, S. L. Xiao, P. J. Ma and G. H. Cui, *Transit. Met. Chem.*, 2013, **38**, 627–633.

115 N. Hussain and V. K. Bhardwaj, *Dalt. Trans.*, 2016, **45**, 7697–7707.

116 X. Y. Wu, H. X. Qi, J. J. Ning, J. F. Wang, Z. G. Ren and J. P. Lang, *Appl. Catal. B Environ.*, 2015, **168**–**169**, 98–104.

117 C. A. Downes and S. C. Marinescu, *J. Am. Chem. Soc.*, 2015, **137**, 13740–13743.

118 C. A. Downes and S. C. Marinescu, *Dalt. Trans.*, 2016, **45**, 19311–19321.

119 C. A. Downes and S. C. Marinescu, *ACS Catal.*, 2017, **7**, 848–854.

120 R. Mishra, E. Ülker and F. Karadas, *ChemElectroChem*, 2017, **4**, 75–80.

121 P. Buchwalter, J. Rosé and P. Braunstein, *Chem. Rev.*, 2015, 115, 28–126.

122 L. K. G. Ackerman, M. M. Lovell and D. J. Weix, *Nature*, 2015, **524**, 454–457.

123 S. Ko, B. Kang and S. Chang, *Angew. Chemie - Int. Ed.*, 2005, **44**, 455–457.

124 K. Griffiths, A. C. Tsipis, P. Kumar, O. P. E. Townrow, A. Abdul-Sada, G. R. Akien, A. Baldansuren, A. C. Spivey and G. E. Kostakis, *Inorg. Chem.*, 2017, **56**, 9563–9573.

125 G. Kumar and R. Gupta, *Chem. Soc. Rev.*, 2013, **42**, 9403.

126 A. M. Kirillov, J. A. S. Coelho, M. V. Kirillova, M. F. C. G. da Silva, D. S. Nesterov, K. R. Gruenwald, M. Haukka and A. J. L. Pombeiro, *Inorg. Chem.*, 2010, **49**, 6390–6392.

127 A. Bhunia, M. A. Gotthardt, M. Yadav, M. T. Gamer, A. Eichhöfer, W. Kleist and P. W. Roesky, *Chem. - A Eur. J.*, 2013, **19**, 1986–1995.

128 M. Yadav, A. Bhunia, S. K. Jana and P. W. Roesky, *Inorg. Chem.*, 2016, **55**, 2701–2708.

129 G. Kumar, G. Kumar and R. Gupta, *RSC Adv.*, 2016, **6**, 21352–21361.

130 Y.-L. Hou, R. W.-Y. Sun, X.-P. Zhou, J.-H. Wang and D. Li, *Chem. Commun.*, 2014, **50**, 2295–2297.

131 N. Kuwamura, Y. Kurioka and T. Konno, *Chem. Commun.*, 2017, **53**, 846–849.